



PII S0016-7037(96)00061-0

Hydrosulphide complexing of Au(I) in hydrothermal solutions from 150–400°C and 500–1500 bar

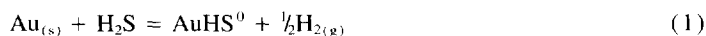
LIANE G. BENNING and TERRY M. SEWARD

Institute for Mineralogy and Petrography, Swiss Federal Institute of Technology, ETH-Zentrum, 8092 Zürich, Switzerland

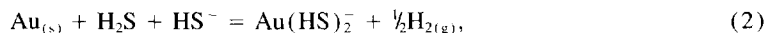
(Received July 6, 1995; accepted in revised form February 15, 1996)

Abstract—The solubility of gold has been measured in aqueous sulphide solutions at temperatures between 150°C and 500°C and pressures of 500–1500 bar over a wide range of pH and total dissolved sulphur concentrations. The solubilities ranged from 0.002–1 mg/kg (1×10^{-8} to 5×10^{-6} m) in experiments with low total sulphur and acid pH, and from 2–108 mg/kg (1×10^{-5} to 5×10^{-4} m) in solutions with high total reduced sulphur concentrations and near neutral pH. The solubilities generally increased with increasing temperature, pH, and total dissolved sulphur. At near neutral pH, an inverse correlation between solubility and pressure was observed, whereas in acid pH solutions, above 150°C, increasing pressure also increased the solubility.

In near neutral pH solutions a solubility maximum was observed. This maximum is due to the species $\text{Au}(\text{HS})_2^-$. However, with increasing temperature, in accordance with the shift of pK_1 of H_2S towards more alkaline pH, the maximum solubility also shifts to higher pH-values and consequently, at high temperatures the species stable at lower pH will dominate. It has been unambiguously proven that over a wide range of temperatures and pressures in reduced sulphur-containing hydrothermal solutions of low pH, the stoichiometry of the dominant Au(I)-hydrosulphide complex, is AuHS^0 . High temperature and high pressure equilibrium constants for the formation of the Au(I)-hydrosulphide complexes, AuHS^0 , and $\text{Au}(\text{HS})_2^-$, pertaining to the equilibria



and



have been calculated. The nonlinear least squares fitted equilibrium constant for reaction (1) varies from $\log K_{(1)} = -6.81$ at 150°C/500 bar to a maximum of -5.90 at 200°C/1500 bar and decreases again at higher temperatures (-7.83 at 400°C/500 bars). For reaction (2), a similar variation occurs: $\log K_{(2)} = -1.45$ at 150°C/500 bar to -1.03 at 250°C/500 bar and -1.75 at 400°C/1500 bar. The thermodynamic functions for the Au(I)-hydrosulphide formation reactions and the cumulative and step-wise formation constants were derived after transforming the above reactions into isocoulombic form.

The equilibrium constants for the uncharged complex, AuHS^0 , show that this species plays an important role in the transport and deposition of gold in ore depositing environments which are characterised by low pH fluids.

1. INTRODUCTION

In order to understand the formation of hydrothermal gold deposits, it is necessary to discern the physicochemical conditions which govern the transport and precipitation mechanisms of gold in hydrothermal solutions. In comparison to other metals, relatively much is known about the hydrothermal chemistry of gold (Seward, 1991). Nevertheless, attempts to quantitatively model the transport and deposition mechanisms are still impeded by a dearth of reliable high temperature and pressure, experimentally based thermodynamic data.

Most experimental studies pertaining to the transport of gold in hydrothermal ore solutions have focused on the role of chloride and reduced sulphur-containing ligands. Gold solubility studies in chloride (e.g., Ogryzlo, 1935; Henley, 1973; Vilor, 1973; Wood et al., 1987; Zotov and Baranova, 1989; Seward, 1991; Gammons and Williams-Jones, 1995) and reduced sulphur-containing solutions (e.g., Ogryzlo, 1935; Zviaginicev and Paulsen, 1940; Weissberg, 1970;

Seward, 1973; Shenberger and Barnes, 1989; Renders and Seward, 1989; Hayashi and Ohmoto, 1991; Pan and Wood, 1994; Gibert et al., 1993; Zotov and Baranova, 1995) have demonstrated that under typical hydrothermal conditions (low oxidation potential, neutral to slightly acid pH), the dominant gold complexing ligands are reduced sulphur species. The stability constants for Au(I) chloride complexes (e.g., at 25°C, see Seward, 1991) are up to twenty orders of magnitude smaller than those of Au(I) hydrosulphide complexes and, therefore, the latter predominate. Despite this observation, the stability constants for Au(I) hydrosulphide complexes in high temperature and high pressure environments are not yet well defined. This is particularly true for the low pH region where no satisfactory data are available.

It is generally accepted that in near neutral pH, reduced sulphur-bearing solutions, the dominant Au(I) hydrosulphide complex is $\text{Au}(\text{HS})_2^-$ (Seward, 1973; Shenberger and Barnes, 1989; Renders and Seward, 1989; Zotov and Baranova, 1995). The stoichiometry of this complex has been firmly established over a wide range of temperatures (from

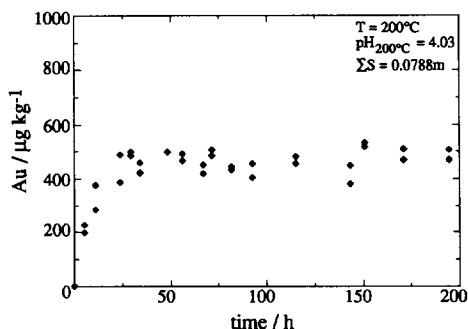


FIG. 1. Total Au solubility ($\mu\text{g}/\text{kg}$) as a function of sampling time (hours) showing the approach to equilibrium from undersaturation for a solution at 200°C and 500 bar. The size of the symbols in all figures represents the precision of the analysis.

25°C to 350°C) and pressures (up to 1000 bar). However, the high temperature equilibrium formation constants for this species from the different studies, vary by up to 1.5 log units. The maximum solubility of Au as $\text{Au}(\text{HS})_2^-$ is found where $\text{pH} = \text{p}K_1$ of H_2S . With increasing temperature, in accordance with the shift of $\text{p}K_1$ of H_2S towards more alkaline pH (Ellis and Giggenbach, 1971; Suleimenov and Seward, 1995), the maximum gold solubility also shifts to higher pH. Consequently, above 300°C the species stable at lower pH will become increasingly important for gold transport.

For the acid pH region, two complexes have been proposed: AuHS^0 and $\text{HAu}(\text{HS})_2^0$. For the neutral species, AuHS^0 , proposed as the stable species at high temperatures by Seward (1973), the stoichiometry and stability constant were clearly determined at 25°C by Renders and Seward (1989). Zotov and Baranova (1995) has conducted experiments at 350°C in acid H_2S bearing solutions and also suggested AuHS^0 as the stable species. The protonated complex, $\text{HAu}(\text{HS})_2^0$, was suggested by Hayashi and Ohmoto (1991) on the basis of experiments in NaCl- and H_2S -bearing aqueous solutions at 250 – 350°C . Gibert et al. (1993) have determined the solubility of Au in KCl solutions at temperatures up to 450°C . From their data, AuHS^0 is likely to be the dominant species. Yet, the discrepancies in the thermodynamic data for the pyrite-pyrrhotite-magnetite assemblage (their oxidation state buffer) made a conclusive determination of the stable species unfeasible, and the formation of $\text{HAu}(\text{HS})_2^0$ could not be ruled out.

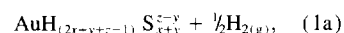
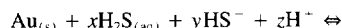
The major goal of this study, therefore, was to determine unambiguously the stoichiometry of the complex responsible for gold transport under high temperature, acid pH conditions, as well as to extend the thermodynamic database for Au(I) hydrosulphide species to higher temperatures and pressures. The bulk of the work concentrated on experiments under acid pH conditions at temperatures between 150 and 400°C and 500–1500 bar. The equilibrium formation constants for the near neutral pH species, $\text{Au}(\text{HS})_2^-$, have been redetermined and are reported here together with equilibrium formation constants for the uncharged complex, predominating at low pH. The aim of this work was also to produce a set of self-consistent thermodynamic data which is independent (as far as possible) of any literature thermodynamic

data. Thus, the reliability of the thermodynamic data derived rests primarily on the uncertainties inherent in these experiments and on the data treatment.

2. EXPERIMENTAL METHODS

2.1. Design

A general equation which describes the equilibria involved in Au(I)-hydrosulphide complex formation by the dissolution of gold in aqueous sulphide solutions may be written



with, $K_{s,xyz}$, the equilibrium constant:

$$K_{s,xyz} = \frac{a_{\text{AuH}_{(2x-y+z-1)}\text{S}_{x+y}^{z-y}} \cdot f_{\text{H}_2}^{0.5}}{a_{\text{H}_2\text{S}}^x \cdot a_{\text{HS}^-}^y \cdot a_{\text{H}^+}^z}. \quad (1b)$$

This reaction conveniently describes the solubility of gold as a function of pH and total reduced sulphur activity. In order to derive the stoichiometry and the equilibrium constants of the dominant Au(I) complexes at a given pressure and temperature, the intensive variables a_{HS^-} , $a_{\text{H}_2\text{S}_{(aq)}}$, and f_{H_2} have to be independently fixed or determined. In this way, the system is completely defined.

For the pH range of interest, three sets of experimental conditions were considered:

- (a) $\text{Au}_{(s)} + \text{H}_2\text{S} + \text{H}_2\text{O} + \text{H}_{2(g)} \quad \text{pH} \approx 4$
- (b) $\text{Au}_{(s)} + \text{H}_2\text{S} + \text{NaHS} + \text{H}_2\text{O} + \text{H}_{2(g)} \quad \text{pH} \approx \text{neutral}$
- (c) $\text{Au}_{(s)} + \text{H}_2\text{S} + \text{H}_3\text{PO}_4 + \text{H}_2\text{O} + \text{H}_{2(g)} \quad \text{pH} < 4.$

In the first two sets, (a) and (b), the pH was controlled by fixing the $\text{H}_2\text{S}/\text{HS}^-$ ratio. In set (c) the pH was adjusted to more acid values by using phosphoric acid. Total reduced sulphur corresponds in set (a) and (c) to the molality of H_2S , while in set (b) the $\text{H}_2\text{S}/\text{HS}^-$ ratio was controlled at near neutral pH by addition of a NaOH solution of known molality. In all three sets, the oxidation potential

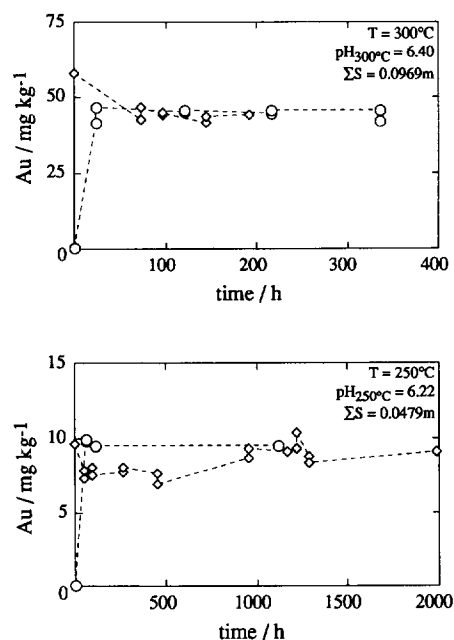


FIG. 2. Total gold (mg/kg) plotted vs. time (hours) showing the approach to equilibrium from under- and supersaturation at (a) 300°C and (b) 250°C ; both experiments were conducted at 500 bar.

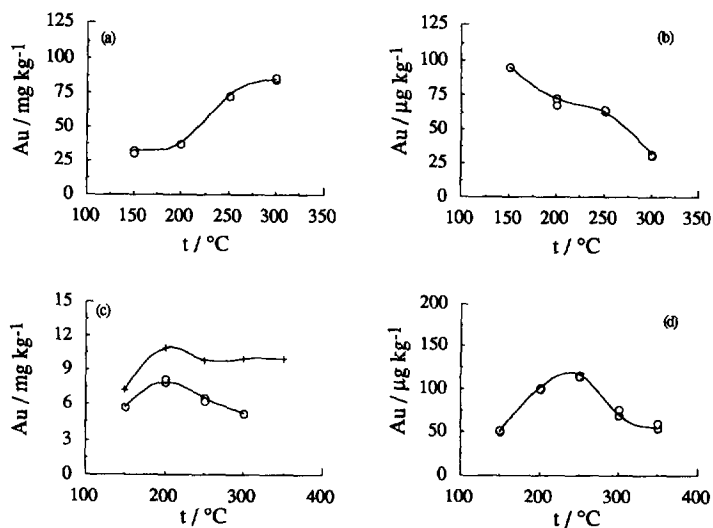


FIG. 3. Variation of gold solubility (mg/kg or $\mu\text{g}/\text{kg}$) with temperature ($^{\circ}\text{C}$) for a number of experiments conducted at a constant pressure of 500 bar: (a) run 22: $\Sigma\text{S} = 0.1133 \text{ m}$, $p_{\text{H}_2} = 0.0357 \text{ bar}$; (b) run 14: $\Sigma\text{S} = 0.0108 \text{ m}$, $p_{\text{H}_2} = 0.0357 \text{ bar}$; (c) run 23: (\circ) $\Sigma\text{S} = 0.0176 \text{ m}$, $p_{\text{H}_2} = 0.0357 \text{ bar}$; run 27 (+) $\Sigma\text{S} = 0.0478 \text{ m}$, $p_{\text{H}_2} = 0.1925 \text{ bar}$; (d) run 16: $\Sigma\text{S} = 0.0786 \text{ m}$, $p_{\text{H}_2} = 0.0357 \text{ bar}$.

was fixed through a known amount of hydrogen gas added directly to the solutions.

2.2 Apparatus, Solution Preparation, and Run Constraints

The experiments were carried out in Bridgman seal-type autoclaves of 300 and 1000 ml internal volume, which contained flexible gold reaction-cell systems. The cells were made of pure gold (99.99%, Johnson Matthey) with a wall thickness of 0.18 mm and a maximum fluid volume of 200 ml and 600 ml, respectively. Pressure tubing ($\frac{1}{4}$ " lined with gold (2.2 mm OD and 0.75 mm wall thickness), connected the reaction cells to the sampling assembly via a titanium valve. The sampling from this valve was made through a teflon plug connected with Teflon tubing to the sampling bottles. In this way, the solution was in contact only with gold, Ti, and Teflon. Temperature and pressure were kept constant to $\pm 1^{\circ}\text{C}$ and ± 5 –10 bar. Temperatures (range 150–500 $^{\circ}\text{C}$) were measured with chromel-alumel thermocouples, in direct contact with the pressure medium (distilled water) surrounding the gold cell. Pressure (500–1500 bar) was monitored using 2000 bar transducers with an accuracy of $\pm 0.15\%$ at the full range output.

Hydrogen gas added to the solutions in the gold cell as an analysed Ar-H₂ mixture, fixed the oxidation potential to a known value. In order to check for possible hydrogen diffusion through the gold cell walls during the experiments, a special sampling set-up for hydrogen was constructed, such that, while the system was held at constant temperature and pressure it was possible to remove a calibrated aliquot of fluid from the gold cell. Subsequently, the fluid was transferred into a gas trap where a separation into a gaseous and aqueous phase occurred due to pressure release. In this way, gold (in the aqueous phase) and hydrogen (in the gas phase) and if required, total reduced sulphur and pH could be measured. Hydrogen was measured using a gas chromatograph (GC) to which the gas trap could be directly connected. The added hydrogen, as well as the hydrogen at pressure and temperature was monitored by replicate GC measurements.

The solutions used in the experiments were prepared from freshly boiled, triply-distilled (in quartz glass) water, which was cooled under oxygen-free (99.996%) N₂. The pure H₂S-solutions (pH \approx 4) were prepared by saturating water with H₂S gas (Messer Griesheim, grade 1.8) at 1 bar. For the H₂S-HS⁻ solutions (neutral to slightly acid), a weighed amount of Analar grade NaOH (dried prior to use

at 130 $^{\circ}\text{C}$ for 1 day) was mixed with triply-distilled water, such that a solution of known NaOH molality was obtained. This solution was subsequently saturated with H₂S gas at 1 bar. For experiments using phosphoric acid (pH at temperature $1.8 < \text{pH}_i < 3.5$), a H₃PO₄ solution, standardised against recrystallised borax, was prepared and added to the H₂S solution already in the gold cell. Total sulphide concentrations of all solutions were measured prior to and at the

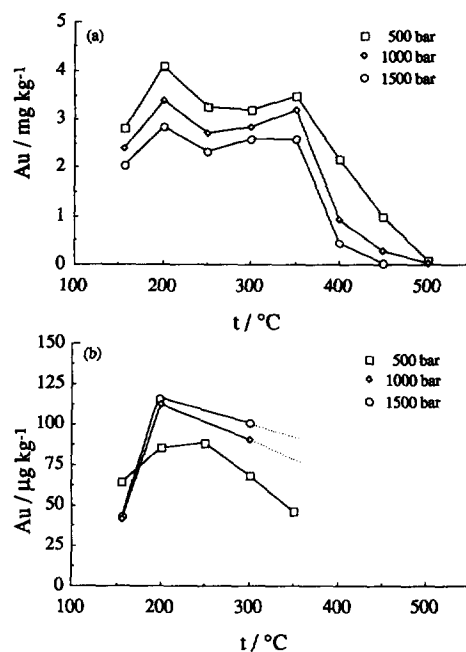


FIG. 4. The effect of pressure on the solubility of gold (mg/kg or $\mu\text{g}/\text{kg}$) plotted as a function of temperature ($^{\circ}\text{C}$). (a) Run 28; pH increases from 5.31 (150 $^{\circ}\text{C}$, 1500 bar) to 6.65 (350 $^{\circ}\text{C}$, 500 bar). (b) Run 20; pH increases from 3.75 (150, 1500 bar) to 4.49 (350 $^{\circ}\text{C}$, 500 bar).

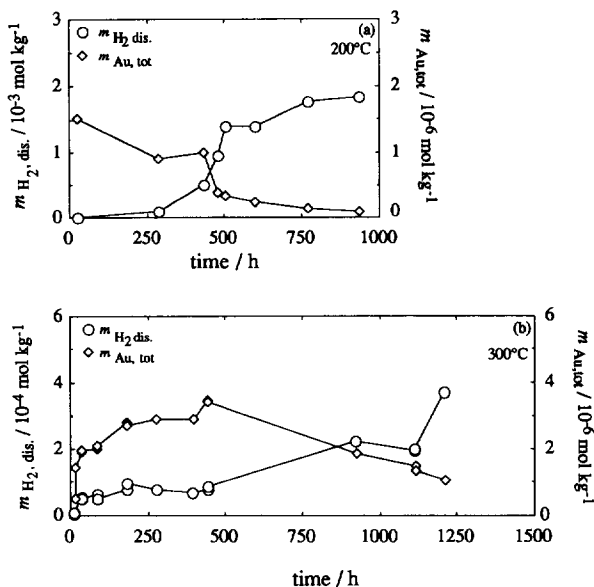


FIG. 5. Molality of hydrogen produced by the disproportionation of H₂S plotted as a function of time and molality of gold in (a) near neutral pH solution at 200°C, 500 bar and ΣS = 0.0822 m and (b) acid pH solution at 300°C, 500 bar and ΣS = 0.0768 m.

end of each run. Starting compositions of all runs are listed in Appendix AI.

Freshly prepared solutions were loaded into the gold cells at 25°C using a small pressure vessel with a separator (movable piston). During solution preparation and loading, considerable care was taken to avoid any oxygen contamination of the solutions in order to prevent the formation of polysulphides or sulphur oxyanions which could affect the gold solubility. The oxidation potential of the system was fixed at a known value by saturating the solutions with hydrogen gas. This was achieved by imposing, at 25°C, a constant partial pressure of an argon-hydrogen mixture (5.5 or 0.55 vpm) to the solution in the gold cell as well as to the pressure medium (water) surrounding the gold cell. At the commencement of these experiments, in order to avoid very low solubilities, especially in the acid pH region, it was necessary to choose adequate hydrogen partial pressures, such that the gold solubilities were not depressed to concentrations which were too difficult to analyse (i.e., < 1 μg/kg).

Samples for gold analysis were extracted while the autoclaves were held at constant pressure and temperature. After discarding the first 1–2 ml, two to five replicate samples were taken. The variance in the gold concentration of replicate samples was usually less than 3–5%. A high variance (up to 15%) occurred when the flow rate of the discharging fluid became too fast, thus causing the fluid to boil during sampling. The samples were weighed and evaporated to dryness, after which the residue was dissolved in aqua regia (to oxidise any remaining sulphur and take the gold in solution). The solutions so obtained were evaporated nearly to dryness and then rediluted with 1 M HCl (30% suprapur®, Merck). The resulting solutions were analysed by an ELAN 5000 (Perkin-Elmer Sciex) ICP-MS or a Varian 840 AAS (precision 2% at a 95% confidence level).

For hydrogen measurements, samples were extracted into a gas mouse (evacuated glass vessels with a septum) which could be connected directly to a gas chromatograph (HP 5890.II). The samples were measured at isothermal conditions, using a 5 m, 5 Å mesh size molecular sieve with nitrogen gas as the carrier. With this method, the absolute volume % of hydrogen in the sampling bottles could be determined, but not the ratio between argon and hydrogen.

The pH of solutions extracted directly from the gold cells was measured, at 25°C, using a PHM 95 pH/ion meter with an Orion Ross combination pH-electrode. High temperature pH values were

calculated using the log K_1 for H₂S and H₃PO₄ listed in Appendix AIII. Total sulphur was determined iodometrically by titration of an acidified, iodine solution (standardised against 0.1 m Na₂S₂O₃ · 5H₂O) with the sample diluted in 1 m NaOH. Immediately after filling the gold cell with solution, three to four titrations (precision ±2–5%) were made at 25°C. During the course of each run, the total sulphur was also monitored; however, the difference between the starting and final values never differed by more than the precision of the analysis.

3. RESULTS

Gold solubilities were measured in aqueous sodium bisulphide and hydrogen sulphide solutions at temperatures from 150–500°C, pressures between 500 and 1500 bar and total sulphur concentrations between 0.11 and 0.02 m. The solubilities range from 0.002–1.1 mg/kg (1.0×10^{-8} to 5.6×10^{-6} m) in experiments with acid pH ($1.8 \leq \text{pH}_i \leq 4.8$), and from 2–108 mg/kg (1.0×10^{-5} to 5.5×10^{-4} m) in experiments with near neutral pH ($5.6 \leq \text{pH}_i \leq 6.8$). The solubility data for more than 400 measurements are listed in Appendix AII.

3.1. Equilibrium

In hydrothermal solubility experiments at high temperatures and pressures, attainment of equilibrium and reversibility of the reactions involved are important requirements. At the beginning of this study, a number of experiments were, therefore, conducted in order to establish criteria for equilibrium and reversibility. Equilibrium gold solubilities, approached from undersaturation, were attained within a few hours at 500°C and up to a maximum of three days at 150°C. For example, in Fig. 1 at 200°C, equilibration approached from undersaturation is achieved in 1.5 days. After reaching a stable value, even if the runs were kept at constant pressure and temperature for up to fifty days, no significant change in solubilities was observed.

The approach to equilibrium solubility from both undersaturation and supersaturation was demonstrated only at $t \geq 250^\circ\text{C}$. At 300°C, equilibrium solubilities were attained from both directions in less than 100 hours (Fig. 2a). At temperatures below 300°C, equilibrium was approached from supersaturation by first equilibrating a solution at 350°C and given pressure and then dropping the temperature to 300°C or lower. The solubilities initially decrease to as much as 25–50% below the equilibrium value obtained by approach from undersaturation. With time, the solubilities increase and reach the equilibrium value approached previously from undersaturation. In Fig. 2b it can be seen that when equilibrium is approached from supersaturation at 250°C, a decrease of nearly 25% occurs. In order to reach the equilibrium solubility previously approached from undersaturation, a time span of seven weeks was required. At $t < 250^\circ\text{C}$, a decrease of up to 50% of the initial undersaturation value was observed and the recovery towards the equilibrium values was much slower. The reason for the undershooting of the equilibrium solubility observed during approach from supersaturation is not yet clear because the kinetics of the involved reactions are at present poorly known. A kinetic study would clarify this problem but this was not the aim of this work. In this study, however, the

final equilibrium constants at $t < 300^\circ\text{C}$ were calculated using only the gold solubility values obtained by approaching equilibrium from undersaturation.

3.2. Temperature Dependence

The variations in gold solubility with temperature for a number of different experimental compositions are plotted in Fig. 3. It can be seen that in the near neutral pH region, at low hydrogen partial pressure and high total reduced sulphur concentration, an increase in gold solubility with increasing temperature is apparent (Fig. 3a). At lower ΣS concentrations, the solubilities are nearly constant over a wide range of temperature but exhibit a maximum at 200°C (Figs. 3c and 4a). By contrast, in most experiments with pure H_2S solutions ($\text{pH} \approx 4$), the solubility decreases with increasing temperature (Fig. 3b). In runs, where the pH is entirely controlled by H_3PO_4 (i.e., $\text{pH} < 3.5$, Fig. 3d), a solubility maximum is found at 200°C to 250°C , similar to the experiments at near neutral pH (Fig. 3c).

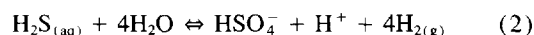
3.3. Pressure Dependence

A number of experiments were also conducted in order to elucidate the effect of pressure on the solubility of gold. In these experiments, equilibrium was approached from undersaturation and from low (500 bar) to high pressure (1500 bar). At 500°C , the experiments were stopped at 1000 bar because of the working limits of the pressure vessels.

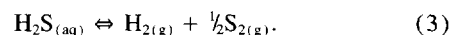
For each temperature/pressure pair, after allowing the system to reach thermal and chemical equilibrium, replicate samples were taken. Equilibration due to pressure change was achieved at a similar time rate as for thermal equilibrium. At near neutral pH, an inverse proportional relationship dominates the gold dissolution; that is, with increasing pressure the solubility drops (Fig. 4a). This effect is constant over the whole range of temperatures ($150\text{--}500^\circ\text{C}$). In Fig. 4a between 350 and 400°C (overstepping the near-critical region of water), a decrease in solubility can be observed, yet the inverse relation with respect to pressure persists. It should be noted, that at 400°C between 500 and 1000 bar, a drastic decrease occurred, which was mainly a consequence of oxidation due to a leak in the gold cell. At acid pH (Fig. 4b), initially, as at near neutral pH (Fig. 4a), an inverse proportional relation to pressure exists but during temperature increase from $150\text{--}200^\circ\text{C}$ an inversion occurs. At 150°C , increasing pressure decreases the solubility, while at temperatures greater than 200°C an increase in pressure leads to an increase in solubility, although between 1000 and 1500 bar the variation is small. To fully understand the influence of pressure at acid pH conditions upon these equilibria, more experiments are necessary. Nevertheless, from these data it is apparent, that in acid pH sulphide solutions, at $t > 150^\circ\text{C}$, a decrease in pressure will favour precipitation, while in near neutral solutions a decrease in pressure will increase the solubility of gold.

3.4. Kinetics of Disproportionation of H_2S

The reactions governing the disproportionation of H_2S in aqueous media can be written as follows:



and



Although it is known that reactions involving aqueous sulphur species proceed rather slowly (Ohmoto and Lasaga, 1982), the $\text{H}_2\text{S}\text{--}\text{HSO}_4^-$ buffer is still often used to fix the redox state of aqueous systems (Shenberger and Barnes, 1989; Hayashi and Ohmoto, 1991).

In order to study the influence of the disproportionation of H_2S on the experiments described in this study, as well as its effect on the $\text{H}_2\text{S}\text{--}\text{HSO}_4^-$ redox buffer in aqueous media at elevated temperatures and pressures, two experiments were conducted using a near neutral pH solution at 200°C and 500 bar and a pure H_2S solutions ($\text{pH} \approx 4$) at 300°C and 500 bar. In these experiments, the same apparatus and experimental set-up as for the gold solubility experiments was used, except that the oxidation potential of the systems was not fixed by addition of H_2 gas. During the experiments, both the hydrogen and the gold concentrations were monitored as the H_2S disproportionation reaction proceeded. It can be demonstrated (Fig. 5a and b) that the equilibration rate for reaction (3) is very slow. At 200°C , for example (Fig. 5a), the experiments were kept at pressure and temperature for up to forty-one days and the redox equilibrium had not been established, that is, the progressive disproportionation of H_2S was still continuing. Similarly at 300°C , equilibrium for the H_2S disproportionation reaction was not achieved even after fifty-two days (Fig. 5b). It should also be kept in mind that the establishment of redox equilibrium between aqueous sulphur species as described by reaction (2) and (3) is also extremely kinetically inhibited (Ohmoto and Lasaga, 1982). Over the time span of our experiments, we were unable to detect the presence of zero-valent sulphur (spectroscopically as polysulphide) or sulphate sulphur in solution. It should be kept in mind, however, that at 300°C (and to a lesser extent at 200°C), polysulphides disproportionate quite rapidly (Giggenbach, 1974). Referring to Fig. 5 and according to reaction (2), it is clear that the amount of sulphate sulphur produced (as HSO_4^-) during the course of the H_2S disproportionation experiments would be small (i.e., $\leq 10^{-4}$ m at 300°C). The H_2S solutions (0.0768 and 0.0822 m) were analysed by iodometric back-titration before and after these experiments and remained constant within the analytical precision of $\pm 2\%$.

These observations emphasize the problem of trying to control or maintain the hydrogen fugacity at a known or constant value in high temperature hydrothermal experiments by assuming attainment of redox equilibrium amongst aqueous sulphur species. An implication of these results is that the use of aqueous sulphur species as an oxidation state buffer is not advised and data up to 300°C collected from experiments where this buffer has been used and where equilibrium solubilities were assumed must be treated with caution.

In this study, the problem has been avoided by working with known, fixed hydrogen concentrations much in excess of those associated with the equilibrium disproportionation of H_2S . In addition, the disproportionation of H_2S was sup-

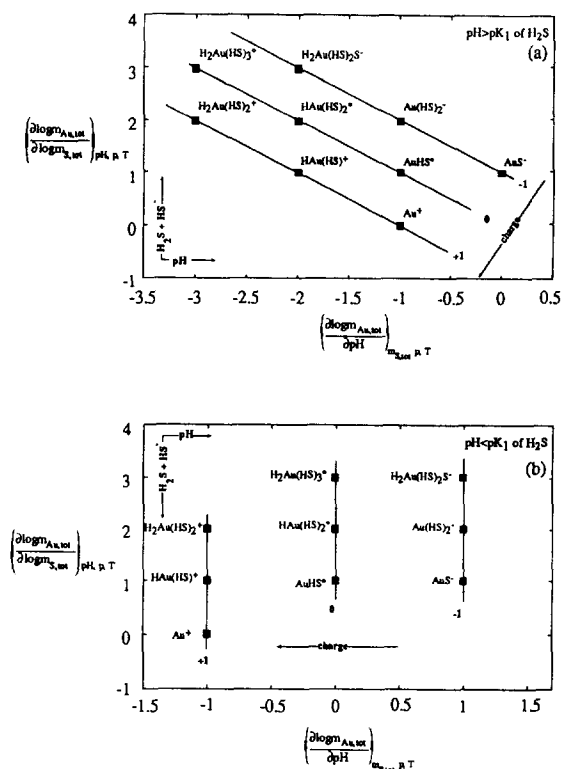


FIG. 6. Some of the possible mononuclear gold (I) hydrosulphide complexes and the slopes for $\log m_{\text{Au,ion}}$ as a function of pH at (a) $\text{pH} > \text{p}K_{1,\text{H}_2\text{S}}$ and (b) $\text{pH} < \text{p}K_{1,\text{H}_2\text{S}}$.

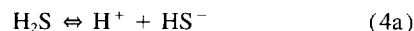
pressed by the added hydrogen. In this way, equilibrium gold solubilities have been obtained without needing to consider the role of side reactions such as (2) and (3). Furthermore, it was not necessary to rely on literature-based thermodynamic data for these reactions in order to calculate equilibrium hydrogen fugacities.

4. SPECIATION

The system studied can be described using three components, gold + sulphide solution + hydrogen gas, and was chosen to be as simple as possible, in order to avoid all potentially unknown or poorly known parameters (like thermodynamic data for solid mineral buffers) which would introduce considerable uncertainties to the final evaluation of the experimental data. In sulphide solutions, the most important sulphur ligand forming stable complexes with Au(I), will be the HS^- species. The other potential sulphur ligand, S^{2-} , is negligible in the range of pH studied (Giggenbach, 1971).

The general dissolution reaction for gold as mononuclear Au(I) hydrosulphide complexes is given by reaction (1a), the equilibrium constant for which being defined by equation (1b). In order to derive the equilibria defining the conditions of gold-hydrosulphide complex formation, the equilibria involving reduced sulphur species and phosphoric acid have to be taken into account. Data for the equilibrium constants used in the calculations are summarized in Appendix AIII. The equilibria with the strongest influence upon the gold-

hydrosulphide equilibrium constants is the ionisation reaction for H_2S :



with the first ionisation constant of H_2S , $K_{1,\text{H}_2\text{S}}$, expressed as:

$$K_{1,\text{H}_2\text{S}} = \frac{a_{\text{HS}^-} \cdot a_{\text{H}^+}}{a_{\text{H}_2\text{S}}} \quad (4b)$$

Data on $\text{p}K_1$ of H_2S are from Ellis and Giggenbach (1971) and have been corrected for pressure effects using the partial molar volume data reported by Ellis and McFadden (1972). The extrapolation of $\text{p}K_1$ of H_2S to temperatures above 276°C was made using a regression method similar to Clarke and Glew (1966). The activity coefficient of H_2S , $\gamma_{\text{H}_2\text{S}}$, was calculated using the values for Henry's law constants for H_2S determined by Suleimenov and Krupp (1994) assuming a Setchenov-type equation that relates the salting coefficient to the true ionic strength of the solution. The hydrosulphide ion activity was corrected for the possibility of ion-pairing with Na^+ at high temperatures and pressures. The data for the NaHS^0 ion pair formation according to the reaction

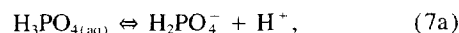


are by analogy with NaCl^0 taken from Shock et al. (1992). Oelkers and Helgeson (1993) have recently discussed the possible role of cluster species in supercritical aqueous solutions. However, the highest Na concentration in these experiments was 0.0373 m (see Appendix AI) but for the majority of solutions in the near neutral pH region, Na concentrations were < 0.01 m. Therefore, only the possible presence of the simple NaHS^0 ion pair was considered. In any event, the correction to the HS^- activity is minor and only applies to the higher temperature-pressure regime of these experiments. In the low pH experiments, no Na was present. The individual ion activity coefficient for HS^- , γ_{HS^-} , was calculated by means of the extended Debye-Hückel equation (Helgeson, 1969),

$$\log \gamma_n = \frac{-A|Z_n|I^{1/2}}{1 + \hat{a}BI^{1/2}} + B^\circ I, \quad (6)$$

where B° is the deviation function at any given temperature, I is the ionic strength (equivalent to m_{HS^-}), Z_n is the charge on species n and \hat{a} is the distance of closest approach which corresponds to the ion size parameters for HS^- , H^+ , Na^+ , and OH^- estimated by analogy with Kielland (1937). The parameters A and B in Eqn. 6 are the conventional molal Debye-Hückel coefficients which are functions of the density ($\rho_{\text{H}_2\text{O}}$) and dielectric constant ($\epsilon_{\text{H}_2\text{O}}$) of water (Haar et al., 1984). Because the ionic strengths were always less than 0.0373 m, activity coefficient corrections are small, and more than adequately considered by application of Eqn. 6.

For the set of experiments in which phosphoric acid was used [set (c)], the pH was fixed at more acidic values through the reaction



for which the first dissociation constant can be expressed as

$$K_{1,H_3PO_4} = \frac{a_{H_2PO_4^-} \cdot a_{H^+}}{a_{H_3PO_4}} \quad (7b)$$

Data for K_{1,H_3PO_4} were taken from Read (1988).

The hydrogen fugacities were calculated from the initial hydrogen concentration, input as a hydrogen-argon mixture, using the Henry's Law constant data in SUPCRT92 (Johnson et al., 1992). These data are based upon those given in Shock et al. (1989) where the high pressure values have been obtained using the partial molar volume data of Tjepel and Gubbins (1972). A small correction was also made for the hydrogen produced by the gold dissolution (i.e., reaction 1a). Hydrogen generated by the disproportionation of H_2S was negligible due to suppression by the added hydrogen-argon mixture.

4.1. Complex Stoichiometries

From Eqn. 1b for any sulphide concentration, the total gold solubility may be defined as a sum of all gold species present in solution

$$m_{Au,tot} = \sum_x \sum_y \sum_z K_{s,xyz} a_{H_2S}^x a_{HS^-}^y a_{H^+}^z f_{H_2}^{-0.5} \gamma_{AuH_{(2x+y+z-1)}S_{x+y}^{-1}} \quad (8)$$

where the maximum coordination of Au(I) is 2.

Combining Eqns. 4a and 4b with the expression for total reduced sulphur,

$$m_{S,tot} = m_{HS^-} + m_{H_2S} \quad (9)$$

it is possible to derive the activities of a_{H_2S} and a_{HS^-} as function only of K_1 of H_2S , pH, and $m_{S,tot}$:

$$a_{HS^-} = \left[\frac{K_{1,H_2S} \cdot \gamma_{H_2S}}{a_{H^+} \cdot \gamma_{HS^-} + K_{1,H_2S} \cdot \gamma_{H_2S}} \right] \cdot m_{S,tot} \cdot \gamma_{HS^-} \quad (10)$$

In order to simplify this equation, the term in brackets is substituted by the function, α , which represents the degree of dissociation of H_2S . Consequently,

$$a_{HS^-} = \alpha \cdot m_{S,tot} \cdot \gamma_{HS^-} \quad (11)$$

and combining Eqns. 4b and 11 we obtain

$$a_{H_2S} = \alpha \cdot m_{S,tot} \cdot \gamma_{HS^-} \cdot a_{H^+} \cdot K_{1,H_2S}^{-1} \quad (12)$$

If Eqns. 11 and 12 are substituted back into Eqn. 1b, an expression for the equilibrium constant which depends only on total gold, fugacity of hydrogen, pH, and total sulphur is obtained. The above mentioned quantities were either measured or calculated from the experiments. The equilibrium constant $K_{s,xyz}$ can, therefore, be expressed as

$$K_{s,xyz} = \frac{a_{AuH_{(2x+y+z-1)}S_{x+y}^{-1}} \cdot f_{H_2}^{0.5}}{[\alpha \cdot m_{S,tot} \cdot \gamma_{HS^-}]^{x+y} \cdot [a_{H^+}]^{x+z} \cdot [K_{1,H_2S}]^{-x}} \quad (13)$$

Combining Eqn. 8 with Eqn. 13, the expression for the total gold concentration can be written as

$$m_{Au,tot} = \sum_x \sum_y \sum_z K_{s,xyz} K_{1,H_2S}^{-x} f_{H_2}^{-0.5} \cdot (\alpha m_{S,tot} \gamma_{HS^-})^{x+y} a_{H^+}^{x+z} \gamma_{AuH_{(2x+y+z-1)}S_{x+y}^{-1}} \quad (14)$$

Taking the logarithm and differentiating Eqn. 14 with respect to total sulphur at constant pH, pressure, and temperature, and with respect to pH at constant $m_{S,tot}$, pressure, and temperature, a set of general equations for the ideal slope of the solubility curves in the $\log m_{S,tot}$ vs. $\log m_{Au,tot}$ and pH vs. $\log m_{Au,tot}$ space is obtained. If pH is constant, the slope can be expressed as

$$\left(\frac{\partial \log m_{Au,tot}}{\partial \log m_{S,tot}} \right)_{pH,p,T} = (x + y) \quad (15)$$

For simplicity, the function, α , may be approximated, such that two regions of pH are identified:

$$\alpha = K_1/a_{H^+} \quad pH < pK_1 \text{ of } H_2S \quad (16a)$$

and

$$\alpha = 1 \quad pH > pK_1 \text{ of } H_2S \quad (16b)$$

Thus, for $pH > pK_1$

$$\left(\frac{\partial \log m_{Au,tot}}{\partial pH} \right)_{m_{S,tot},p,T} = -(x + z) \quad (17a)$$

and for $pH < pK_1$

$$\left(\frac{\partial \log m_{Au,tot}}{\partial pH} \right)_{m_{S,tot},p,T} = y - z \quad (17b)$$

In this way, any mononuclear Au(I) hydrosulphide complex defined by reaction (1a) will be described by three equations (15, 17a, and 17b) which define it uniquely in the delineated fields. The graphical technique to identify the possible Au(I) hydrosulphide complexes is shown in Fig. 6a and 6b, where vertical axes represent a stepwise addition of $H_2S + HS^-$ and horizontal axes give the stepwise addition of H^+ ions.

At this point it should be noted that in comparison to Seward (1973) and Renders and Seward (1989), the slopes in $pH > pK_1$ of H_2S and $\log m_{Au,tot}$ vs. $\log m_{S,tot}$ space differ by a half a log unit. This arises from the different forms of Eqn. 8, bearing in mind that Seward (1973) measured the solubility of elemental gold in equilibrium with a pyrite + pyrrhotite redox buffer assemblage and Renders and Seward (1989) equilibrated sulphide solutions with Au_2S rather than $Au_{(s)}$.

As discussed in the introduction, in this work three possible species were primarily of interest: $Au(HS)_2^-$, $HAu(HS)_2^0$, and $AuHS^0$. In the pH region studied ($2 \leq pH \leq 7$), the presence of $Au(HS)_2^-$ is quite well documented from 25°C to high temperatures (Renders and Seward, 1989; Seward, 1973; Shenberger and Barnes, 1989). However, a major aim was to determine whether $AuHS^0$ or $HAu(HS)_2^0$ or any other species occurred in high temperature low pH sulphide solutions.

The stoichiometry of species contributing to the measured solubility has been verified both graphically and using a nonlinear least squares approach. For the graphical approach,

Table 1. Ideal slopes for the species of interest as function of pH and total sulphur in the delineated pH regions

species	$\left(\frac{\partial \log m_{\text{Au,tot}}}{\partial \text{pH}}\right)_{m_{\text{S,tot}}, p, T}$		$\left(\frac{\partial \log m_{\text{Au,tot}}}{\partial \log m_{\text{S,tot}}}\right)_{\text{pH}, p, T}$	x, y, z from equation (1a)
	pH < pK _{1,H₂S}	pH > pK _{1,H₂S}		
	(y-z)	-(x+z)	(x+y)	
Au(HS) ₂ ⁻	1	-1	2	1, 1, 0
HAu(HS) ₂ ⁰	0	-2	2	2, 0, 0
AuHS ⁰	0	-1	1	1, 0, 0

the ideal slopes of the three species discussed above are given in Table 1 as a function of pH and total sulphur concentration. Due to the fact that at $\text{pH} > \text{p}K_{1,\text{H}_2\text{S}}$, the stable species is $\text{Au}(\text{HS})_2^-$ and that at $\text{pH} < \text{p}K_{1,\text{H}_2\text{S}}$, the two neutral species have the same slope (zero), it is obvious that a graphical determination of the stable species at $\text{pH} < \text{p}K_{1,\text{H}_2\text{S}}$ can only be made by using the slopes in the $\log m_{\text{Au,tot}}$ vs. $\log m_{\text{S,tot}}$ space (Fig. 6b). In such a plot, the ideal slope for the species AuHS^0 is +1, whereas a slope of +2 would indicate the protonated species $\text{HAu}(\text{HS})_2^0$. Figure 7 shows the experimental results at $\text{pH} \approx 4$ plotted in $\log m_{\text{Au,tot}}$ vs. $\log m_{\text{S,tot}}$ space. The data which are spread over a wide range of total sulphur concentrations show that the slope of the best fit line for temperatures from 150–300°C is near unity. This demonstrates clearly that the complex, AuHS^0 , is the stable species in low pH sulphide solutions.

From the graphical approach, it was concluded that in acid and near neutral pH solutions, the dominant Au(I) hydrosulphide complexes are AuHS^0 and $\text{Au}(\text{HS})_2^-$, respectively. Initial estimates for the equilibrium constants for AuHS^0 were previously reported (Benning and Seward, 1994, 1995).

The stoichiometry of both species contributing to the observed solubility was unambiguously determined using a nonlinear least squares fitting approach similar to that used by Renders and Seward (1989). The final equilibrium constants for the formation of AuHS^0 and $\text{Au}(\text{HS})_2^-$, as well as their associated uncertainties were calculated using the nonlinear least squares routine in which all the data at a given temperature and pressure were treated simultaneously. In addition various other schemes of species (e.g., $\text{HAu}(\text{HS})_2^0 + \text{Au}(\text{HS})_2^-$) were also tested but the scheme which statisti-

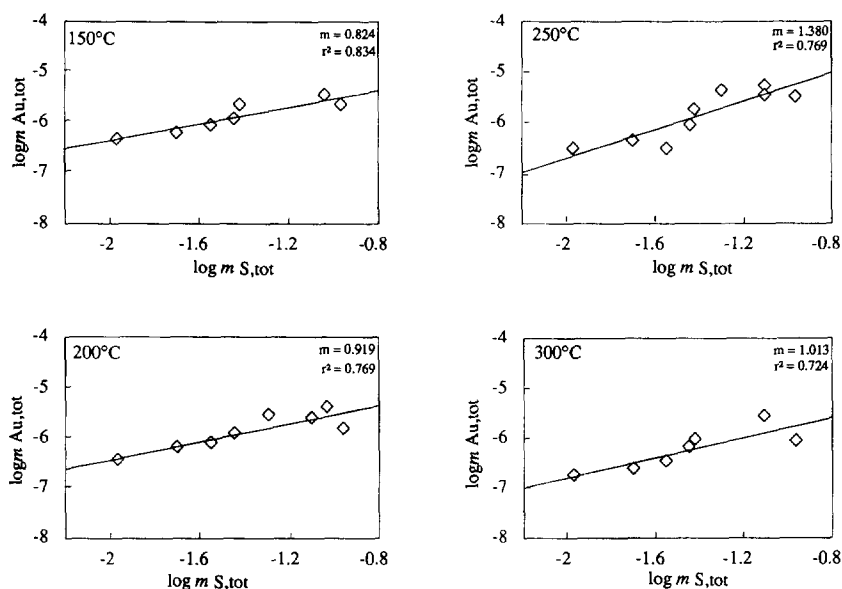


Fig. 7. The solubility of gold, $\log m_{\text{Au,tot}}$, at 150–300°C (500 bar) at $\text{pH} \approx 4$, as a function of $\log m_{\text{S,tot}}$; the points represent average run values for samples collected at the same temperature. The lines are best fit lines with slopes close to one, indicating that the species AuHS^0 is the stable species under these conditions.

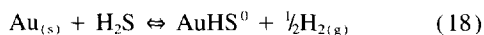
TABLE 2. Equilibrium constants, $K_{s,xyz}$, for the species AuHS^0 and $\text{Au}(\text{HS})_2^-$ at 500, 1000 and 1500 bar pressure pertaining to equations (18) and (19). Because of the smaller data base, equilibrium constants and their associated uncertainties for 400°C and for 1000 and 1500 bar have been calculated directly from the solubility data without using the nonlinear least squares routine.

	log $K_{s,xyz}$					
	150°C	200°C	250°C	300°C	350°C	400°C
$K_{s,100}$ at 500 bar	-6.81 (0.51)	-6.17 (0.04)	-6.06 (0.12)	-6.39 (0.11)	-6.67 (0.14)	-7.83 (0.20)
$K_{s,100}$ at 1000 bar	-6.35 (0.11)	-5.96 (0.06)	-6.03*	-6.30 (0.04)	-7.00 (0.20)	-7.65*
$K_{s,100}$ at 1500 bar	-6.30 (0.03)	-5.90 (0.12)	-5.90*	-6.22 (0.09)	-6.81*	-7.62*
$K_{s,110}$ at 500 bar	-1.45 (0.04)	-1.09(0.06)	-1.03 (0.05)	-1.14 (0.06)	-1.35 (0.11)	-1.52 (0.15)
$K_{s,110}$ at 1000 bar	-1.09 (0.05)	-1.08 (0.10)	-1.20 (0.07)	-1.34 (0.08)	-1.45 (0.10)	-1.63*
$K_{s,110}$ at 1500 bar	-1.12 (0.05)	-1.10 (0.10)	-1.27 (0.03)	-1.42 (0.05)	-1.53(0.05)	-1.75*

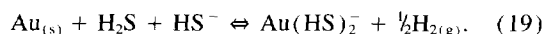
* interpolated / extrapolated

cally best fitted the solubility data using the nonlinear least squares procedure was $\text{AuHS}^0 + \text{Au}(\text{HS})_2^-$. The final equilibrium constants were calculated using this model which gave the best minimized sum of squares.

The high temperature equilibrium constants, $K_{s,100}$ and $K_{s,110}$ for the formation of AuHS^0 and $\text{Au}(\text{HS})_2^-$, respectively, pertain to the equilibria



and



Data for $K_{s,100}$ for reaction (18) and $K_{s,110}$ for reaction (19) at 500, 1000, and 1500 bar are given in Table 2. It should be noted, that uncertainties for the equilibrium constants calculated using a nonlinear least squares routine represent confidence intervals calculated at 95% probability.

5. DISCUSSION

5.1. Thermodynamics of Complex Formation

At this point we have established that two Au(I) hydrosulphide complexes account for the solubility of gold in high pressure and high temperature sulphide-containing hydrothermal solutions. Maximum gold solubility is obtained at $\text{pH} = \text{p}K_1$ of H_2S and is due to the complex $\text{Au}(\text{HS})_2^-$. The equilibrium constants determined for this species at 1000 bar are in good agreement (within 0.25 log units) with those of Seward (1973) but differ by up to 0.75 log units from those of Shenberger and Barnes (1989) for saturated water vapour pressure and are highly discrepant (up to 1.5–2 log units) with those of Pan and Wood (1994). However, a direct comparison to the literature data can not be made until a conversion to the same standard state conditions is carried out (see later). At low pH and high temperatures, the pres-

ence of the neutral complex AuHS^0 has been unambiguously proven. This confirms the data of Renders and Seward (1989) who determined the stoichiometry and stability of this species at 25°C, but contradicts the high temperature results of Hayashi and Ohmoto (1991) who proposed the protonated species $\text{HAu}(\text{HS})_2^0$. However, the large scatter in the data of Hayashi and Ohmoto (1991) makes a conclusive determination of the stoichiometry of the dominant complex somewhat doubtful.

Experimentally derived equilibrium constants provide a basis for the derivation of standard thermodynamic properties at any given pressure and temperature. However, it should be kept in mind that solubility measurements are a less accurate method for determining precise thermodynamic quantities than for example calorimetry, and errors can be incorporated into the calculations (especially for ΔC_p° and ΔV°).

Initially, all thermodynamic functions were derived by fitting the equilibrium constants for reaction (18) and (19) to pressure and temperature dependent equations of the form given by Eqn. 24. From these equations, the equilibrium constants at saturated water vapour pressures ($swvp$) were derived (Table 3) and are plotted in Fig. 8 together with the experimentally derived equilibrium constants. It should be noted that although the extrapolation is far over extended (see Fig. 9), the 25°C values are nevertheless in reasonable agreement with the experimentally derived equilibrium constants of Renders and Seward (1989) who determined log $K_{s,100}$ and log $K_{s,110}$ to be -11.14 , and -5.54 , respectively.

The equilibrium constants for $\text{Au}(\text{HS})_2^-$ from Seward (1973) and the log $K_{s,110}$ from Table 4 (both at 1000 bar) are in excellent agreement (Fig. 9a). However, in Fig. 9b it can be seen that the equilibrium constant for the species $\text{Au}(\text{HS})_2^-$, log $K_{s,110}$ at saturated water vapour pressure when plotted together with the $swvp$ data from Shenberger and

TABLE 3. Equilibrium constants, $K_{s,xyz}$, for AuHS^0 and $\text{Au}(\text{HS})_2^-$ at saturated water vapour pressure referring to equations (18) and (19).

	25°C	150°C	200°C	250°C	300°C	350°C
$\log K_{s,100}$ at swvp	-11.47	-7.14	-6.46	-6.24	-6.40	-6.92
$\log K_{s,110}$ at swvp	-5.89	-1.56	-1.07	-0.94	-1.05	-1.28

Barnes (1989) and Pan and Wood (1994) show fairly large discrepancies. The reason for the discrepancies with Shenberger and Barnes (1989) is, however, not easily explained because the same standard state conditions apply and similar chemical systems were studied. The only feasible explanation could lie in the problems arising from the disproportionation of H_2S . It was shown previously (see Results) that equilibrium in systems where the sulphate-sulphide redox buffer is used is attained at a very slow rate. Shenberger and Barnes (1989) were aware of this problem and thus used data only from experiments involving the sulphide-sulphate redox equilibria at temperatures above 250°C. However, as seen previously, the attainment of equilibrium with this re-

dox couple is achieved very slowly even at temperatures as high as 300°C (see Fig. 5b).

As for the species AuHS^0 , only meager data are available with which to compare. Hayashi and Ohmoto (1991) suggested on the basis of gold solubility experiments in NaCl- and H_2S containing aqueous solutions at 250–350°C that the species $\text{HAu}(\text{HS})_2^0$ is the stable stoichiometry. Gibert et al. (1993) measured the solubility of gold in 0.5 m KCl solutions at 350–450°C with the pH buffered by the quartz-muscovite-K-feldspar assemblage and sulphur and hydrogen buffered by the pyrite-pyrrhotite-magnetite assemblage and favoured the species AuHS^0 as the stable complex. Zotov

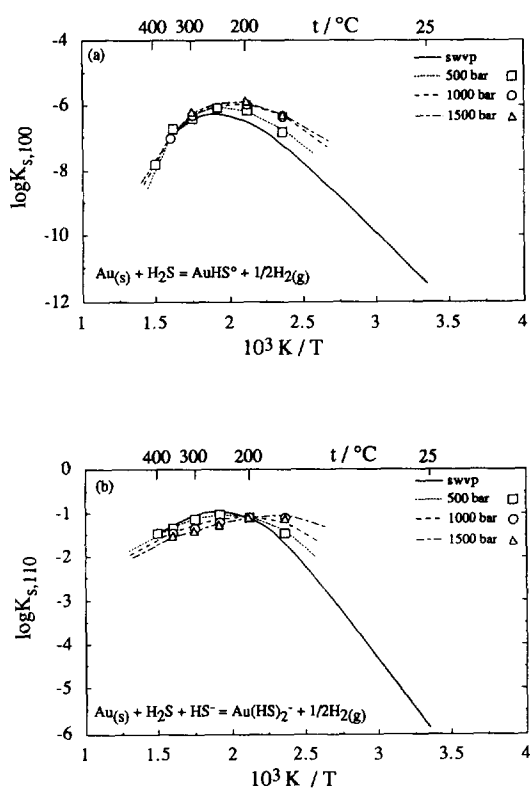


FIG. 8. Equilibrium constants, $K_{s,xyz}$, for the species AuHS^0 (a) and $\text{Au}(\text{HS})_2^-$ (b) referring to Eqns. 18 and 19 plotted as a function of inverse temperature (in Kelvin) from saturated water vapour pressure to 1500 bar. The symbols delineate the experimentally derived equilibrium constants, while the lines represent the fitted equations.

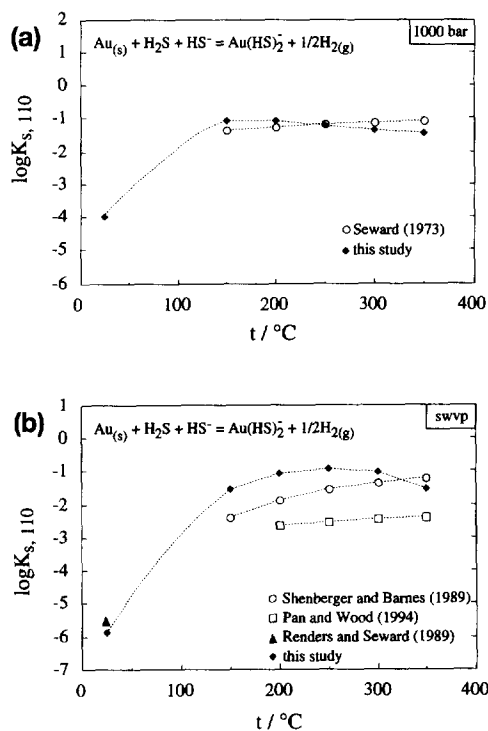


FIG. 9. Equilibrium constants, $K_{s,110}$ for reaction (19) for the species $\text{Au}(\text{HS})_2^-$ plotted as a function of temperature (°C): (a) at 1000 bar, open circles: Seward (1973); filled diamonds: this study (the 25°C point is an extrapolated value at 1000 bar); the difference between the two datasets is just slightly larger than the experimental uncertainties; (b) at saturated water vapour pressure: open circles, Shenberger and Barnes (1989); squares: Pan and Wood (1994); filled triangle at 25°C: Renders and Seward (1989); filled diamonds: this study.

TABLE 4. Equilibrium constants, K_{xyz} , for the species AuHS^0 and $\text{Au}(\text{HS})_2^-$ referring to reactions (21) and (22) from saturated water vapour pressure to 1500 bar.

	log K_{xyz}					
	150°C	200°C	250°C	300°C	350°C	400°C
AuHS⁰						
swvp	11.36	9.38	7.48	5.53	3.52	-
500 bar	11.48	9.51	7.51	5.44	3.70	1.29
1000 bar	11.96	9.73	7.62	5.53	3.35	1.28
1500 bar	12.03	9.81	7.71	5.61	3.42	1.18
Au(HS)₂⁻						
swvp	16.82	14.50	12.51	10.76	9.18	-
500 bar	16.84	14.59	12.54	10.68	9.02	7.60
1000 bar	17.22	14.61	12.38	10.49	8.90	7.50
1500 bar	17.21	14.61	12.32	10.41	8.82	7.26

and Baranova (1995) measured gold solubilities in aqueous H_2S solutions and determined the equilibrium constant at 350°C in terms of AuHS^0 . All these results interpreted in terms of AuHS^0 are plotted in Fig. 10. It is clear that the different sets are in disagreement with the log $K_{s,100}$ values for AuHS^0 derived in the present study by 0.5 (Zotov, 1994) and up to 2 log units (Gibert et al., 1993). Uncertainties in the thermodynamic data for the mineral assemblages used by Gibert et al. (1993) may explain a difference of up to 0.2–0.5 log units. Another reason for the differing values is the use of the H_2S ionisation constant data from the SUPCRT92 database (Johnson et al., 1992), whereas we have used values based on Ellis and Giggenbach (1971).

The first ionisation constant of H_2S is fundamental for the calculation of the equilibrium constants for the gold dissolution reaction. At high temperatures, a comparison of the pK_1

of H_2S values calculated using the SUPCRT92 database with the extrapolated pK_1 of H_2S values used in this study (Appendix AIII), shows a difference of up to more than 1 log unit. Ellis and Giggenbach (1971) determined the first ionisation constants for H_2S up to 276°C at saturated vapour pressure. These data were corrected for pressure effects using the partial molar volume data of Ellis and McFadden (1972) and extrapolated to higher temperatures (Appendix AIII). New, preliminary spectroscopic data for pK_1 of H_2S (Suleimenov and Seward, 1995) are, up to 300°C, in reasonable agreement with the data of Ellis and Giggenbach (1971). For the time being and until a more complete and accurate dataset for $t > 300^\circ\text{C}$ becomes available, the equilibrium constants for hydrosulphidogold(I) complexes presented in this study are calculated with the pK_1 of H_2S based on data from Ellis and Giggenbach (1971) which are listed in Appendix AIII. The strong curvature at high temperatures shown in Fig. 8, is, however, mainly a consequence of the involved reactions being highly non-isocoulombic. Ion-solvent interactions influence strongly the heat capacity and volume changes and, therefore, for the final calculation of the thermodynamic properties, reactions (18) and (19) were transformed into isocoulombic and pseudo-isocoulombic reactions. It is well known that much of the dramatic change in the thermodynamic functions (especially ΔC_p° and ΔV° for a given equilibrium reaction) can be removed by representing such reactions in an isocoulombic form (Lindsay, 1980). By definition, a true isocoulombic reaction has to have the same number of reactants and charges as the products, while for a pseudo-isocoulombic reaction, the number of reactants and products may differ but the nature of the charges on both sides of the reaction has to be the same. For reactions (18) and (19), this transformation was made by applying the gold redox reaction

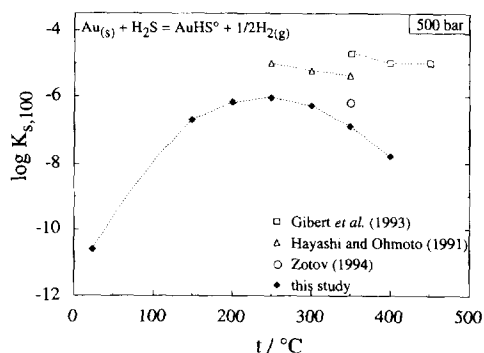
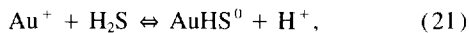


FIG. 10. Equilibrium constants, $K_{s,100}$ [reaction (18)], for the species AuHS^0 plotted as a function of temperature ($^\circ\text{C}$) at 500 bar pressure; open circle: Zotov (1994); squares: Gibert et al. (1993); triangles: Hayashi and Ohmoto (1991) reinterpreted in terms of AuHS^0 ; filled diamonds: this study (the 25°C data point is extrapolated).



The equilibrium constants for reaction (20) taken from the SUPCRT92 database (Johnson et al., 1992) are listed in Appendix AIII and are consistent with the 25°C data of Latimer (1952) and Bjerrum (1948). Using this approach, the experimental gold solubilities in hydrosulphide solutions can be recalculated in terms of the reactions



The transformed equilibrium constants, $\log K_{100}$ and $\log K_{110}$ together with the fitted equilibrium constants for the formation of AuHS^0 and $\text{Au}(\text{HS})_2^-$ extrapolated to 25°C and saturated water vapour pressure (*swvp*) are listed in Table 4 and plotted against inverse temperature in Fig. 11.

The molar Gibbs free energy of these reactions can be calculated at each temperature and pressure directly from the equilibrium constants by applying

$$\Delta G^\circ = -RT \ln K. \quad (23)$$

In order to calculate the other thermodynamic functions, the equilibrium constants, $\log K_{xyz}$, for AuHS^0 and $\text{Au}(\text{HS})_2^-$ from Table 4 were fitted to equations of the type

$$\log K = A + Bp + \frac{C}{T} + DT + ET^2, \quad (24)$$

where p is in bars, T is in Kelvin and C , D , and E are in

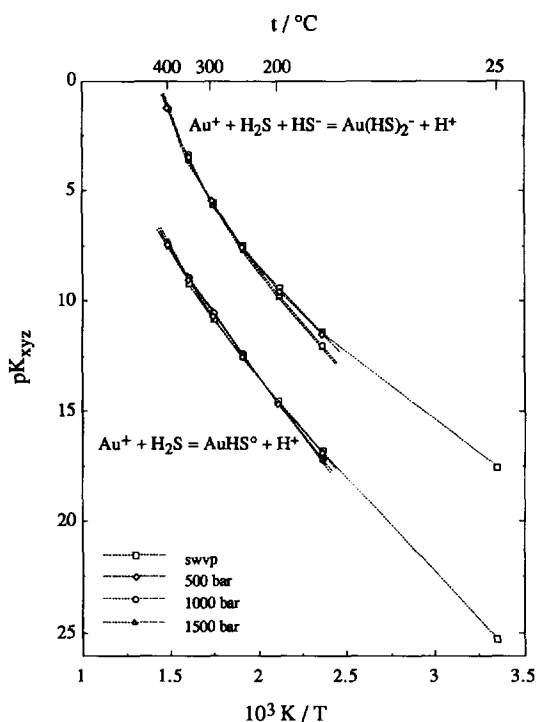


FIG. 11. Equilibrium constants, K_{xyz} , for the species AuHS^0 and $\text{Au}(\text{HS})_2^-$ referring to Eqns. 21 and 22 plotted as a function of inverse temperature (in Kelvin). The equilibrium constants show a linear dependence up to about 250°C as expected for isocoulombic reactions; however, at temperatures above 250°C, a slight curvature is obvious. This is in agreement with the behaviour of isocoulombic reactions (Lindsay, 1980).

TABLE 5. Coefficients for equation (24) used to fit the equilibrium constants, K_{xyz} , for AuHS^0 and $\text{Au}(\text{HS})_2^-$ from TABLE 4.

parameter	coefficients for AuHS^0
A	-9.4663
B	-12.840E-04
C = (x+y·p)	(6264.3925 + 74.681E-02·p)
D = (x+y·p)	(34.30E-03 - 10.943E-03·p)
E = (x+y·p)	-47.439E-06
Σ deviation ²	0.29
stand. deviation	0.16

parameter	coefficients for $\text{Au}(\text{HS})_2^-$
A	4.6410
B	-16.355E-04
C = (x+y·p)	(7113.3819 + 80.743E-02·p)
D = (x+y·p)	-10.943E-03
E = (x+y·p)	0
Σ deviation ²	0.28
stand. deviation	0.09

p is pressure in bars

turn pressure dependent functions of the type $(x + yp)$. There could be some discussion about the best (or better) choice of fitting equations. However, due to the lack of any experimental heat capacity data, the choice of the fitting equation was based totally on the goodness of fit, although an overfitting was avoided. Values for the coefficients of Eqn. 24 are given in Table 5.

The first derivative of Eqn. 24, with respect to temperature at constant pressure, provides values for the enthalpy change, ΔH° , at any given temperature and pressure, while from the second derivative, the heat capacity change, ΔC_p° , can be obtained. In turn, entropy changes, ΔS° , may be derived in the conventional way, using the enthalpy and the free energy values. The following equations apply:

for ΔH° :

$$\left(\frac{\partial \log K}{\partial T} \right)_p = \frac{\Delta H^\circ}{2.303RT^2} \quad (25a)$$

$$\Delta H^\circ = 2.303 \cdot R(DT^2 + 2ET^3 - C), \quad (25b)$$

for ΔS° :

$$\Delta G^\circ = -RT \ln K = \Delta H^\circ - T\Delta S^\circ \quad (26a)$$

$$\Delta S^\circ = \frac{\Delta H^\circ - \Delta G^\circ}{T}, \quad (26b)$$

and for ΔC_p° :

$$\left(\frac{\partial^2 \ln K}{\partial T^2} \right)_p = \left(\frac{\partial \Delta H^\circ}{\partial T} \right)_p = \Delta C_p^\circ \quad (27a)$$

$$\Delta C_p^\circ = 2.303 \cdot R(2DT + 6ET^2). \quad (27b)$$

The isothermal pressure dependence of the equilibrium constants permits the evaluation of the partial molar volume change, $\Delta \bar{V}^\circ$ for reactions (21) and (22). This can be ex-

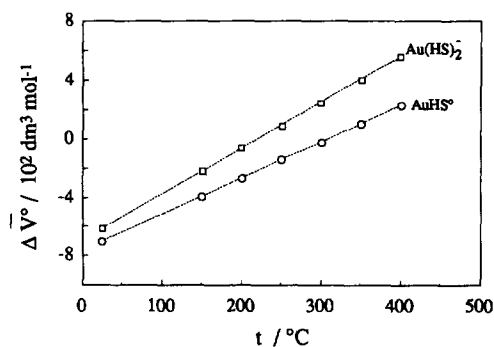


FIG. 12. Isobaric temperature dependence of the standard partial molar volume change for the complexes, AuHS^0 (reaction 21) and $\text{Au}(\text{HS})_2^-$ (reaction 22).

pressed as the first derivative of the equilibrium constants with respect to pressure,

$$\left(\frac{\partial \ln K}{\partial p}\right)_T = \frac{-1}{RT} \left(\frac{\partial \Delta G^\circ}{\partial p}\right)_T = \frac{-\Delta \bar{V}^\circ}{RT}, \quad (28)$$

combined with Eqn. 24 and the nil coefficients from Table 5, this becomes:

$$\Delta \bar{V}^\circ = 0.74681pR - BRT \quad \text{for } \text{AuHS}^0 \quad (29a)$$

and

$$\Delta \bar{V}^\circ = 0.80743pR - BRT \quad \text{for } \text{Au}(\text{HS})_2^-. \quad (29b)$$

The second derivative of the equilibrium constant with respect to pressure at constant temperature gives the partial molar isothermal compressibility change, $\Delta \bar{\kappa}^\circ$,

$$\Delta \bar{\kappa}^\circ = \left(\frac{\partial^2 \ln K}{\partial p^2}\right)_T = -\left(\frac{\partial \Delta \bar{V}^\circ}{\partial p}\right)_T. \quad (30)$$

However, in the model employed, the compressibility is pressure independent and hence zero. Therefore, the change in partial molar volume for reactions (21) and (22) is pressure independent but shows a positive linear correlation with temperature (Fig. 12). It should be kept in mind that from the statistical point of view, Eqn. 24 gave a satisfactory fit to the data but, even though the absolute values for $\Delta \bar{V}^\circ$

TABLE 6. Thermodynamic functions for reactions (21) and (22) from 25 to 400°C and from swvp to 1500 bar based on the fitted values for $\log K_{xyz}$ from equation (24).

t/°C	ΔG°		ΔH°		ΔS°		ΔC_p°		$\Delta \bar{V}^\circ$	
	AuHS^0	$\text{Au}(\text{HS})_2^-$	AuHS^0	$\text{Au}(\text{HS})_2^-$	AuHS^0	$\text{Au}(\text{HS})_2^-$	AuHS^0	$\text{Au}(\text{HS})_2^-$	AuHS^0	$\text{Au}(\text{HS})_2^-$
swvp										
25	-100.2	-144.1	-109.7	-154.8	-32	-36	-93	-125	-7.0	-6.0
150	-92.0	-136.3	-140.1	-173.8	-114	-89	-420	-177	-3.9	-2.2
200	-85.0	-131.3	-165.6	-183.3	-170	-110	-599	-198	-2.7	-0.6
250	-74.8	-125.3	200.9	-194.1	-241	-132	-804	-219	-1.4	0.9
300	-60.7	-118.1	-147.5	-206.3	-326	-154	-1038	-240	-0.2	2.5
350	-42.0	-109.5	-306.9	-220.1	-425	-177	-1298	-261	1.0	4.1
400	-17.2	-98.3	-383.7	-238.8	-544	-209	-1585	-282	2.3	5.6
500 bar										
25	-103.7	-147.1	-116.9	-162.5	-44	-52	-93	-125	-7.0	-6.0
150	-93.9	-137.4	-147.2	-181.4	-126	-104	-420	-177	-3.9	-2.2
200	-86.3	-131.7	-172.5	-190.8	-182	-125	-599	-198	-2.7	-0.6
250	-75.5	-124.9	-207.4	-201.2	-252	-146	-804	-219	-1.4	0.9
300	-60.8	-117.1	-253.4	-212.7	-336	-167	-1038	-240	-0.2	2.5
350	-41.6	-108.2	-311.7	-225.3	-433	-188	-1298	-261	1.0	4.1
400	-17.2	-98.3	-383.7	-238.8	-544	-209	-1585	-282	2.3	5.6
1000 bar										
25	-107.1	-150.2	-124.0	-170.3	-57	-67	-93	-125	-7.0	-6.0
150	-95.9	-138.5	-154.3	-189.2	-138	-120	-420	-177	-3.9	-2.2
200	-87.6	-132.0	-179.7	-198.5	-195	-141	-599	-198	-2.7	-0.6
250	-76.2	-124.4	-214.6	-209.0	-265	-162	-804	-219	-1.4	0.9
300	-60.9	-115.8	-260.6	-220.5	-348	-183	-1038	-240	-0.2	2.5
350	-41.1	-106.2	-318.9	-233.0	-446	-204	-1298	-261	1.0	4.1
400	-16.1	-95.5	-390.8	-246.6	-557	-2245	-1585	-282	2.3	5.6
1500 bar										
25	-110.6	-153.2	-131.2	-178.0	-69	-83	-93	-125	-7.0	-6.0
150	-97.8	-139.6	-161.4	-196.9	-150	-135	-420	-177	-3.9	-2.2
200	-88.9	-132.3	-186.8	-206.3	-207	-156	-599	-198	-2.7	-0.6
250	-76.9	-124.0	-221.8	-216.7	-277	-177	-804	-219	-1.4	0.9
300	-61.0	-114.6	-267.7	-228.2	-361	-198	-1038	-240	-0.2	2.5
350	-40.6	-104.1	-326.0	-240.7	-458	-219	-1298	-261	1.0	4.1
400	-15.0	-92.6	-398.0	-254.3	-569	-240	-1585	-282	2.3	5.6

Units: ΔG° and ΔH° in kJ mol^{-1} ; ΔS° and ΔC_p° in $\text{J mol}^{-1}\text{K}^{-1}$; $\Delta \bar{V}^\circ$ in $10^2 \text{ dm}^3 \text{ mol}^{-1}$ ($=10 \text{ cm}^3 \text{ mol}^{-1}$)

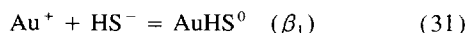
TABLE 7. Cumulative and stepwise formation constants for AuHS⁰ and Au(HS)₂⁻ at saturated water vapour pressure referring to equations (31), (32) and (33).

	25°C	150°C	200°C	250°C	300°C	350°C
log β ₁	24.55(0.3)	18.17(0.3)	16.58(0.2)	15.08(0.2)	13.53(0.2)	11.83(0.3)
log β ₂	32.32(0.3)	23.64(0.3)	21.70(0.3)	20.12(0.2)	18.76(0.3)	17.49(0.3)
log K ₂	7.68(0.3)	5.47(0.2)	5.12(0.2)	5.04(0.3)	5.23(0.3)	5.66(0.2)

(Table 6) may inherit fairly large errors, the positive correlation of ΔV^0 with temperature will persist. In Table 7, the calculated values for the thermodynamic functions are listed from 25–400°C and *swvp* to 1500 bar.

5.2. Cumulative and Stepwise Formation Constants

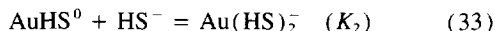
The cumulative and stepwise formation constants for the gold species AuHS⁰ and Au(HS)₂⁻ (β₁, β₂ and K₂), have been calculated by combining the equilibrium constants for H₂S from Appendix AIII with the *swvp* values for the equilibrium constants of the Au(I) hydrosulphide complexes obtained in this study (Table 4). The values for the cumulative and stepwise formation constants listed in Table 7 refer to the equilibria



and



from which the stepwise formation constant for the reaction:



can be calculated. The 25°C value derived in this study (Table 7) for log β₁ = 24.55 for the uncharged AuHS⁰ complex is in excellent agreement with that reported by Renders and Seward (1989) of log β₁ = 24.5. The value of log β₂ = 32.32 is consistent with, but nevertheless somewhat discrepant with respect to the more reliable value of log β₂ = 30.1 given by Renders and Seward (1989).

In order to derive the thermodynamic functions for the formation constants from Table 7, a procedure similar to the one applied to the experimentally derived equilibrium

constants (Eqns. 24–30) was applied. The form of the equation of the type

$$\text{Log } K = A + BT + CT^2 + D/T + E \ln T \quad (34)$$

(*T* in Kelvin) which best fitted the formation constants involved four terms. The coefficients for Eqn. 34 to which the formation constants were fitted are given in Table 8 and the calculated thermodynamic functions are listed in Table 9.

Gold has the electronic configuration, Xe 4f¹⁴5d¹⁰6s¹. The Au⁺ ion with filled 5d shells is a typical class 'b' metal ion or soft Lewis acid. This classification of ion-ligand interactions is rather simplistic but, nevertheless, helps in understanding the selectivity of Au⁺ towards some ligands. As the archetype soft electron acceptor, Au⁺ forms preferentially more stable complexes with more polarizable soft Lewis bases (e.g., I⁻, HS⁻). Complex formation at 25°C between class 'b' metal ions and ligands is enthalpy dominated such that the free energy of reaction is mainly a function of the ΔH^0 term and the entropy of the reaction is less important. In a soft-soft interaction, in order to replace water dipoles from the hydration shells during the formation of a complex, an exothermic enthalpy change is required. The formation of AuHS⁰ at 25°C is accompanied by a large energy release ($\Delta H^0 = -135.6 \text{ kJ mol}^{-1}$) and a small positive entropy change ($\Delta S^0 = 15.1 \text{ J mol}^{-1} \text{ K}^{-1}$). With increasing temperature, up to 200–250°C, the ΔH^0 of formation for AuHS⁰ is rather insensitive to temperature but at higher temperatures the contribution of the enthalpy term in the Gibbs free energy becomes more negative and the entropy, after passing a maximum at 150°C decreases rapidly. In the case of Au(HS)₂⁻, the larger, positive entropies and enthalpies at high temperatures suggest that with increasing temperature, the electrostatic interaction between metal cat-

TABLE 8. Coefficients for equation (34) used to fit the formation constants for AuHS⁰ and Au(HS)₂⁻ from TABLE 7.

	A	B	C	D
β ₁	-42.77211	11.646E-02	-97.096E-06	12290.6849
K ₂	13.27821	-42.926E-03	45.368E-06	944.35945

TABLE 9. Thermodynamic functions derived from equilibrium formation constants for AuHS⁰ and Au(HS)₂⁻ at saturated water vapour pressure from 25 to 350°C

t/°C	ΔG°		ΔH°		ΔS°		ΔC_p°	
	(31)	(33)	(31)	(33)	(31)	(33)	(31)	(33)
25	-140.1	-46.1	-135.6	-45.1	15	-4	339	-27
150	-147.2	-44.3	-117.7	-33.6	70	25	-110	238
200	-150.2	-46.4	-129.9	-18.1	43	59	-386	389
250	-151.1	-50.5	-157.3	5.7	-12	107	-719	567
300	-148.5	-57.4	-202.7	39.0	-95	168	-1100	770
350	-141.1	-67.6	-269.0	83.2	-205	241	-1550	999

Units: ΔG° and ΔH° in kJ mol⁻¹; ΔS° and ΔC_p° in J mol⁻¹K⁻¹.

ion and ligand increases as observed for metal chloride complexes at elevated temperatures (Seward, 1981).

5.3. Conclusions and Implications to Gold Transport and Deposition

The main purpose of this work was to obtain a set of thermodynamically consistent data which describe the behaviour of gold in aqueous sulphide solutions. The derived stability constants for the complexes AuHS⁰ and Au(HS)₂⁻ (Table 2) can be used to quantitatively model the transport of gold in natural hydrothermal fluids and to help understand the mechanisms and conditions of gold deposition from hydrothermal fluids in ore-depositing environments. It was shown that in sulphide solutions at near neutral pH, the complex Au(HS)₂⁻ is the dominant gold species. The solubility of gold reaches a maximum where pH = pK₁ of H₂S. However, with increasing temperatures the pK₁ of H₂S shifts towards more alkaline values (Ellis and Giggenbach, 1971; Suleimenov and Seward, 1995) and, therefore, the maximum solubility due to this species also shifts to more alkaline pH. In acid pH, high temperature solutions, the neutral species AuHS⁰, therefore, will be the dominant gold transporting species and although the gold solubility may be 1–2 orders of magnitude lower than at pH > pK₁(H₂S), this complex has to be taken in account when such systems are modelled. For example, in high sulphidation epithermal ore systems (e.g., Arribas et al., 1995) the AuHS⁰ species may play an important role in gold transport and deposition.

The mechanisms involved in gold precipitation include temperature and pressure changes, phase separation, oxidation, sulphide phase precipitation, pH changes, and fluid-wallrock reactions. It is never only one factor which causes gold to precipitate from the transporting solution but a mixture of interdependent factors which are different from deposit to deposit. The main reasons for decreasing the solubility of gold in high temperature sulphide solutions are because of changes in pH and/or total reduced sulphur concentrations. In ore depositing systems, this is achieved by wall rock interaction, oxidation of the fluids (e.g., mixing with meteoric- or seawater), boiling with loss of the volatile components (H₂S, H₂, CO₂) or precipitation of sulphide miner-

als. A temperature and pressure decrease is often assumed to cause precipitation. The effect of temperature on the solubility of gold in sulphide solutions is very strongly related to the total sulphur concentration and the hydrogen fugacity. In systems where high sulphur and low hydrogen fugacities occur, decreasing temperature may play an important role in the precipitation. Experimentally, it can be shown that in acid pH solutions, a decrease in pressure will favour the precipitation of gold from solution, whereas in near neutral solutions, a drop in pressure will increase the solubility of gold, and, therefore, precipitation will be impeded (Fig. 4). However, this effect is probably only important in the near neutral region.

Acknowledgments—This research is based on the Ph.D. thesis of the first author which was supported by the Research Program of the Swiss Federal Institute of Technology. We are grateful to P. Richner and S. Wiget from Section 31 of the EMPA for the help with the ICP-MS measurements. We thank our colleagues B. W. Mountain, O. M. Suleimenov, and J. K. Hovey for many helpful discussions and assistance with computing. We are also grateful to G. M. Anderson, J. B. Fein, C. A. Heinrich, G. R. Helz, D. C. McPhail, G. A. Pal'yanova, and V. A. Pokrovskii for critical comments which helped improve the various versions of the manuscript.

Editorial handling: S. A. Wood

REFERENCES

- Arribas A., Jr., et al. (1995) Geology, geochronology, fluid inclusion, and isotope geochemistry of the Rodalquilar Au-alunite deposit, Spain. *Econ. Geol.* **90**, 795–822.
- Benning L. G. and Seward T. M. (1994) Hydrosulphide complexes of gold(I) at high pressures and temperatures: equilibrium and kinetic problems. *Mineral. Mag.* **58A**, 75–76.
- Benning L. G. and Seward T. M. (1995) AuHS⁰—An important gold-transporting complex in high temperature hydrosulphide solutions. In *Water-Rock Interaction-8* (ed. Y. K. Kharaka, O. V. Chudakov), pp. 783–786. Balkema Press.
- Bjerrum N. (1948) La stabilité des chlorures d'or. *Soc. Chimie Belge Bull.* **57**, 432–445.
- Clarke E. C. W. and Glew D. N. (1966) Evaluation of thermodynamic functions from Equilibrium Constants. *Trans. Faraday Soc.* **62**, 539–547.
- Ellis A. J. and Giggenbach W. (1971) Hydrogen sulphide ionisation and sulphur hydrolysis in high temperature solution. *Geochim. Cosmochim. Acta* **35**, 247–260.
- Ellis A. J. and McFadden I. M. (1972) Partial molal volumes of

- ions in hydrothermal solutions. *Geochim. Cosmochim. Acta* **36**, 413–426.
- Gammons C. H. and Williams-Jones A. E. (1995) The solubility of Au-Ag alloy + AgCl in HCl/NaCl solutions at 300°C: New data on the stability of Au(I) chloride complexes in hydrothermal solutions. *Geochim. Cosmochim. Acta* **59**, 3453–3468.
- Gibert F., Pascal M.-L., and Pichavant M. (1993) Solubility of gold in KCl (0.5m) solution under hydrothermal conditions (350–450°C, 500 bar) (abstr.). In *Proc. 4th International Symposium on Hydrothermal reactions* (ed. M. Cuney and M. Cathelineau), pp. 65–68. Institut Lorrain des Geoscience
- Giggenbach W. F. (1971) Optical spectra of high alkaline sulphide solutions and the second dissociation constant of hydrogen sulphide. *Inorg. Chem.* **10**, 1333–1338.
- Giggenbach W. F. (1974) Equilibria involving polysulfide ions in aqueous sulfide solutions up to 240°C. *Inorg. Chem.* **13**, 1724–1730.
- Haar L., Gallagher J. S., and Kell G. S. (1984) *NBS/NRC Steam tables. Thermodynamic and transport properties and computer programs for vapour and liquid states of water in SI units*. Hemisphere Publ. Corp.
- Hayashi K.-I. and Ohmoto H. (1991) Solubility of gold in NaCl- and H₂S bearing aqueous solutions at 250–350°C. *Geochim. Cosmochim. Acta* **55**, 2111–2126.
- Helgeson H. C. (1969) Thermodynamics of hydrothermal systems at elevated temperatures and pressures. *Amer. J. Sci.* **267**, 729–804.
- Henley R. W. (1973) Solubility of gold in hydrothermal chloride solutions. *Chem. Geol.* **11**, 73–87.
- Johnson J. W., Oelkers E. H., and Helgeson H. C. (1992) SUPCRT92: A software package for calculating the standard molal thermodynamic properties of minerals, gases, aqueous species, and reactions from 1 to 5000 bar and 0°C to 1000°C. *Computers Geosci.* **18**, 899–947.
- Kielland J. (1937) Individual activity coefficients of ions in aqueous solutions. *J. Amer. Chem. Soc.* **59**, 1675–1679.
- Latimer W. M. (1952) *The Oxidation States of the elements and their Potentials in Aqueous Solutions*. Prentice-Hall.
- Lindsay W. T., Jr. (1980) Estimation of concentration quotients for ionic equilibria in high temperature water: the model substance approach. *Proc. Intl. Water Conf.* **41**, 284–294.
- Marshall W. L. and Franck E. U. (1981) Ion product of water substance, 0–1000°C, 1–10,000 bar. New international formulation and its background. *J. Phys. Chem. Ref. Data* **10**, 295–304.
- Oelkers E. H. and Helgeson H. C. (1993) Calculation of dissociation constants and the relative stability of polynuclear clusters of 1:1 electrolytes in hydrothermal solutions at supercritical pressures and temperatures. *Geochim. Cosmochim. Acta* **57**, 2673–2697.
- Ogryzlo S. P. (1935) Hydrothermal experiments with gold. *Econ. Geol.* **30**, 400–424.
- Ohmoto H. and Lasaga A. C. (1982) Kinetics of reactions between aqueous sulfates and sulfides in hydrothermal systems. *Geochim. Cosmochim. Acta* **46**, 1727–1745.
- Pan P. and Wood S. A. (1994) The solubility of Pt and Pd sulfides and Au metal in bisulfide solutions. II. Results at 200–350°C and at saturated vapour pressure. *Mineral. Deposita* **29**, 373–390.
- Read A. J. (1988) The first ionisation constant from 25 to 200°C and 2000 bar for Othophosphoric acid. *J. Sol. Chem.* **17**, 213–224.
- Renders P. J. and Seward T. M. (1989) The stability of hydrosulphido- and sulphido complexes of Au(I) and Ag(I) at 25°C. *Geochim. Cosmochim. Acta* **53**, 244–253.
- Seward T. M. (1973) Thio complexes of gold in hydrothermal ore solutions. *Geochim. Cosmochim. Acta* **37**, 379–399.
- Seward T. M. (1981) Metal complex formation in aqueous solutions at elevated temperatures and pressures. In *Physics and Chemistry of the Earth. Nobel Symposium on the Chemistry and Geochemistry of Solutions at high temperature and pressures* (ed. F. Wickman and D. Rickard), pp. 113–133. Pergamon
- Seward T. M. (1991) The hydrothermal geochemistry of gold. In *Gold metallogeny and exploration* (ed. R. P. Foster), pp. 37–62. Blackie.
- Shenberger D. M. and Barnes H. L. (1989) Solubility of gold in aqueous sulfide solutions from 150 to 350°C. *Geochim. Cosmochim. Acta* **53**, 269–278.
- Shock E. L., Helgeson H. C., and Sverjensky D. A. (1989) Calculation of the thermodynamic and transport properties of aqueous species at high pressures and temperatures: Standard partial molal properties of inorganic neutral species. *Geochim. Cosmochim. Acta* **53**, 2157–2183.
- Shock E. L., Oelkers E. H., Johnson J. W., Sverjensky D. A., and Helgeson H. C. (1992) Calculation of the thermodynamic and transport properties of aqueous species at high pressures and temperatures: Effective electrostatic radii, dissociation constants and standard partial molal properties to 1000°C and 5 kbar. *J. Chem. Soc. Faraday Trans.* **88**, 803–826.
- Suleimenov O. M. and Krupp R. E. (1994) Solubility of hydrogen sulphide in pure water and in NaCl solutions, from 20 to 320°C and at saturation pressures. *Geochim. Cosmochim. Acta* **58**, 2433–2444.
- Suleimenov O. M. and Seward T. M. (1995) Spectrophotometric determination of the first ionisation constant of hydrogen sulphide at high temperatures. In *Water-Rock Interaction-8*. (ed. Y. K. Kharaka and O. V. Chudaev), pp. 113–115. Balkema Press.
- Tiepel E. W. and Gubbins K. E. (1972) Partial molal volumes of gases dissolved in electrolyte solutions. *J. Phys. Chem.* **76**, 3044–3049.
- Vilor N. V. (1973) Laboratory and theoretical data on gold and silica in hydrochemical process. Candidate thesis, Inst. Zemnoy Kory SO AN SSSR, Irkutsk.
- Weissberg B. G. (1970) Solubility of gold in hydrothermal alkaline sulfide solutions. *Econ. Geol.* **65**, 551–556.
- Wood S. A., Crerar D. A., and Borcsik M. P. (1987) Solubility of the assemblage pyrite-pyrrhotite-magnetite-sphalerite-galena-Au-stibnite-bismuthinite-argentite-molybdenite in H₂O-NaCl-CO₂ solutions from 200° to 350°C. *Econ. Geol.* **82**, 1864–1887.
- Zotov A. V. and Baranova N. N. (1989) Thermodynamic features on the aurochloride solute complex, AuCl₂⁻, at temperatures of from 350 to 500°C and under pressure of from 500 to 1500 bar. *Sci. Géol. Bull.* **42**, 335–342.
- Zotov A. V. and Baranova N. N. (1995) The solubility of Au₂S and AuAgS in near-neutral sulphide solutions at temperatures of 25 and 80°C and pressures of 1 and 500 bars. In *Water-Rock Interaction-8* (ed. Y. K. Kharaka and O. V. Chudaev), pp. 773–776. Balkema Press.
- Zotov A. V., Akinfiev N. N., Baranova N. N., and Livin K. A. (1993) Experimental and thermodynamic study of Au(I) and Ag(I) aqueous species at 25–450°C and 1–1500 bar. *Proc. 4th Intl. Symp. Hydrotherm. Reactions*. (unpubl. abstr.).
- Zviaginicev O. E. and Paulsen I. A. (1940) Contribution to the theory of formation of vein gold deposits. *Dokl. Akad. Nauk SSSR* **26**, 647–651.

APPENDIX AI. Starting composition of the runs classified according to the initial input conditions. The runs 01 to 20 H₂S are experiments with pure H₂S and H₂S + H₃PO₄ solutions; runs 21 to 28 are experiments where the pH is adjusted to near neutral values by addition of NaOH.

Run	*Σ S	*H ₃ PO ₄	**H ₂ (gas)	Run	*Σ S	*H ₃ PO ₄	**H ₂ (gas)
01 H ₂ S	0.0505	-	0.03575	16 H ₂ S	0.0753	0.00860	0.03575
02 H ₂ S	0.0788	-	0.03575	17 H ₂ S	0.0953	0.14400	0.03575
03 H ₂ S	0.0919	-	0.03575	18 H ₂ S	0.0216	0.00280	0.03575
04 H ₂ S	0.1094	-	0.03575	19 H ₂ S	0.0326	0.00069	0.03575
05 H ₂ S	0.0201	-	0.03575	20 H ₂ S	0.0786	0.00700	0.03575
06 H ₂ S	0.0361	-	0.03575				
07 H ₂ S	0.0916	-	0.03575	Run	*Σ S	*NaOH	**H ₂ (gas)
08 H ₂ S	0.0383	-	0.03575	21 H ₂ S / HS ⁻	0.1141	0.03730	0.03575
09 H ₂ S	0.0283	-	0.03575	22 H ₂ S / HS ⁻	0.1133	0.03592	0.03575
10 H ₂ S	0.0450	0.00175	0.03575	23 H ₂ S / HS ⁻	0.0176	0.02510	0.03575
11 H ₂ S	0.0066	0.00105	0.03575	24 H ₂ S / HS ⁻	0.0992	0.00623	0.19250
12 H ₂ S	0.0655	0.00098	0.03575	25 H ₂ S / HS ⁻	0.0969	0.00750	0.19250
13 H ₂ S	0.0242	0.01080	0.03575	26 H ₂ S / HS ⁻	0.1012	0.00675	0.37400
14 H ₂ S	0.0108	-	0.03575	27 H ₂ S / HS ⁻	0.0479	0.00380	0.19250
15 H ₂ S	0.0412	0.00871	0.03575	28 H ₂ S / HS ⁻	0.0280	0.00230	0.19250

* molalities
** bar

Appendix AII. Experimental solubility data; the data in this table refer to the stated temperatures and pressures; the run numbers in this table are the same as those in Appendix I.

H2S or H2S/H3PO4 150°C							H2S or H2S/H3PO4 200°C						
run	Au(ppm)	mAu	aH2S	aHS-	fH2,tot	pH	run	Au(ppm)	mAu	aH2S	aHS-	fH2,tot	pH
4.1	0.422	2.1E-06	0.109	1.53E-04	0.0331	3.81	1.1	0.524	2.66E-06	0.0505	7.06E-05	0.0238	4.15
4.2	0.355	1.8E-06	0.109	1.53E-04	0.0331	3.81	1.3	0.615	3.12E-06	0.0505	7.06E-05	0.0237	4.15
4.3	0.516	2.6E-06	0.109	1.53E-04	0.0335	3.81	1.4	0.599	3.04E-06	0.0505	7.06E-05	0.0241	4.15
4.5	0.322	1.6E-06	0.109	1.53E-04	0.033	3.81	1.6	0.605	3.07E-06	0.0505	7.06E-05	0.0241	4.15
4.6	0.429	2.2E-06	0.109	1.53E-04	0.0333	3.81	1.8	0.593	3.01E-06	0.0505	7.06E-05	0.0243	4.15
							1.9	0.575	2.92E-06	0.0505	7.06E-05	0.0241	4.15
5.2	0.15	7.6E-07	0.02	6.55E-05	0.0325	4.18	1.10	0.587	2.98E-06	0.0505	7.06E-05	0.0242	4.15
							1.11	0.576	2.92E-06	0.0505	7.06E-05	0.0241	4.15
6.1	0.239	1.2E-06	0.036	8.79E-05	0.0327	4.06	1.12	0.517	2.62E-06	0.0505	7.06E-05	0.0239	4.15
6.2	0.224	1.1E-06	0.036	8.79E-05	0.0327	4.06	1.14	0.566	2.87E-06	0.0505	7.06E-05	0.024	4.15
							2.1	0.483	2.45E-06	0.0788	8.82E-05	0.0237	4.05
7.2	0.625	3.2E-06	0.092	1.40E-04	0.0337	3.85	2.2	0.498	2.53E-06	0.0788	8.82E-05	0.0239	4.05
7.3	0.738	3.7E-06	0.092	1.40E-04	0.0338	3.85	2.3	0.459	2.33E-06	0.0788	8.82E-05	0.0238	4.05
7.4	0.722	3.7E-06	0.092	1.40E-04	0.0341	3.85	2.5	0.496	2.52E-06	0.0788	8.82E-05	0.0238	4.05
7.5	0.737	3.7E-06	0.092	1.40E-04	0.0341	3.85	2.6	0.499	2.53E-06	0.0788	8.82E-05	0.0237	4.05
7.6	0.741	3.8E-06	0.092	1.40E-04	0.0342	3.85	2.7	0.492	2.50E-06	0.0788	8.82E-05	0.0239	4.05
7.7	0.637	3.2E-06	0.092	1.40E-04	0.0339	3.85	2.8	0.467	2.37E-06	0.0788	8.82E-05	0.0239	4.05
							2.9	0.504	2.56E-06	0.0788	8.82E-05	0.0239	4.05
8.2	0.436	2.2E-06	0.038	9.05E-05	0.0332	4.04	2.10	0.482	2.45E-06	0.0788	8.82E-05	0.0238	4.05
8.3	0.435	2.2E-06	0.038	9.05E-05	0.0333	4.04	2.11	0.445	2.26E-06	0.0788	8.82E-05	0.0238	4.05
8.4	0.451	2.3E-06	0.038	9.05E-05	0.0333	4.04	2.14	0.454	2.30E-06	0.0788	8.82E-05	0.0238	4.05
							2.15	0.478	2.43E-06	0.0788	8.82E-05	0.0237	4.05
9.2	0.167	8.5E-07	0.028	7.78E-05	0.0325	4.11	2.16	0.454	2.30E-06	0.0788	8.82E-05	0.0237	4.05
9.3	0.163	8.3E-07	0.028	7.78E-05	0.0325	4.11	2.17	0.448	2.27E-06	0.0788	8.82E-05	0.0238	4.05
9.4	0.168	8.5E-07	0.028	7.78E-05	0.0325	4.11	2.20	0.515	2.61E-06	0.0788	8.82E-05	0.0238	4.05
							2.21	0.51	2.59E-06	0.0788	8.82E-05	0.0238	4.05
10.1	0.043	2.2E-07	0.045	8.57E-06	0.0322	2.95	2.22	0.469	2.38E-06	0.0788	8.82E-05	0.0238	4.05
10.2	0.048	2.4E-07	0.045	8.57E-06	0.0322	2.95	2.23	0.505	2.56E-06	0.0788	8.82E-05	0.0236	4.05
10.4	0.041	2.1E-07	0.045	8.57E-06	0.0322	2.95	2.24	0.469	2.38E-06	0.0788	8.82E-05	0.024	4.05
							2.26	0.466	2.37E-06	0.0788	8.82E-05	0.0239	4.05
11.1	0.141	7.2E-07	0.066	1.82E-05	0.0324	3.11							
11.2	0.148	7.5E-07	0.066	1.82E-05	0.0325	3.11	3.2	0.873	4.43E-06	0.0919	9.53E-05	0.0246	4.02
							3.3	0.747	3.79E-06	0.0919	9.53E-05	0.0244	4.02
12.1	0.159	8.1E-07	0.066	1.93E-05	0.0325	3.14	3.4	0.785	3.99E-06	0.0919	9.53E-05	0.0245	4.02
12.2	0.153	7.8E-07	0.066	1.93E-05	0.0325	3.14							
12.3	0.184	9.3E-07	0.066	1.93E-05	0.0326	3.14	4.1	0.277	1.41E-06	0.1094	1.04E-04	0.0233	3.98
12.4	0.184	9.3E-07	0.066	1.93E-05	0.0326	3.14	4.2	0.331	1.68E-06	0.1094	1.04E-04	0.0235	3.98
							5.1	0.111	5.64E-07	0.0201	4.44E-05	0.0231	4.35
13.1	0.0055	2.8E-08	0.024	1.39E-06	0.032	2.43	5.2	0.122	6.19E-07	0.0201	4.44E-05	0.0245	4.35
13.2	0.005	2.5E-08	0.024	1.39E-06	0.032	2.43	5.3	0.131	6.65E-07	0.0201	4.44E-05	0.0233	4.35
13.3	0.0046	2.3E-08	0.024	1.39E-06	0.032	2.43							
14.1	0.095	4.8E-07	0.011	4.80E-05	0.0323	4.32	6.1	0.202	1.03E-06	0.0361	5.96E-05	0.0233	4.22
14.2	0.095	4.8E-07	0.011	4.80E-05	0.0323	4.32	6.2	0.265	1.35E-06	0.0361	5.96E-05	0.0234	4.22
14.3	0.09	4.6E-07	0.011	4.80E-05	0.0323	4.32							
14.4	0.091	4.6E-07	0.011	4.80E-05	0.0323	4.32	9.1	0.161	8.17E-07	0.0283	5.28E-05	0.0232	4.28
							9.2	0.165	8.38E-07	0.0283	5.28E-05	0.0232	4.28
16.1	0.048	2.4E-07	0.075	2.44E-06	0.0322	2.49	10.1	0.09	4.57E-07	0.045	5.29E-06	0.0232	3.05
16.2	0.051	2.6E-07	0.075	2.44E-06	0.0322	2.49	10.2	0.089	4.52E-07	0.045	5.29E-06	0.0231	3.05
16.3	0.055	2.8E-07	0.075	2.44E-06	0.0322	2.49	10.3	0.09	4.57E-07	0.045	5.29E-06	0.023	3.05
16.4	0.047	2.4E-07	0.075	2.44E-06	0.0322	2.49							
16.5	0.052	2.6E-07	0.075	2.44E-06	0.0322	2.49	11.1	0.229	1.16E-06	0.0661	1.10E-05	0.023	3.20
							11.2	0.244	1.24E-06	0.0661	1.10E-05	0.0233	3.20
17.1	0.058	2.9E-07	0.095	7.06E-07	0.0321	1.85	11.3	0.239	1.21E-06	0.0661	1.10E-05	0.0234	3.20
17.2	0.069	3.5E-07	0.095	7.06E-07	0.0321	1.85	11.4	0.219	1.11E-06	0.0661	1.10E-05	0.023	3.20
18.1	0.0086	4.4E-08	0.022	1.46E-06	0.0321	2.81	12.1	0.305	1.55E-06	0.0655	1.14E-05	0.0235	3.22
							12.2	0.365	1.85E-06	0.0655	1.14E-05	0.0236	3.22
19.1	0.0096	4.9E-08	0.033	6.21E-06	0.0321	3.26	12.3	0.321	1.63E-06	0.0655	1.14E-05	0.0235	3.22
19.2	0.01	5.1E-08	0.033	6.21E-06	0.0321	3.26							
							13.1	0.0016	8.12E-09	0.0242	9.20E-07	0.0229	2.56
20.1	0.064	3.2E-07	0.079	2.85E-06	0.0322	2.54	13.2	0.0022	1.12E-08	0.0242	9.20E-07	0.0229	2.56
20.2	0.049	2.5E-07	0.079	2.85E-06	0.0322	2.54							

APPENDIX AII. Continued.

150°C	1000 bar						14.1	0.072	3.66E-07	0.0108	3.40E-05	0.0229	4.48
						14.2	0.068	3.45E-07	0.0108	3.40E-05	0.0229	4.48	
20.1	0.039	2E-07	0.079	1.52E-06	0.0321	2.45							
20.2	0.04	2E-07	0.079	1.52E-06	0.0321	2.45	15.1	0.016	8.12E-08	0.0412	1.80E-06	0.0229	2.62
20.3	0.036	1.8E-07	0.079	1.52E-06	0.0321	2.45	15.2	0.013	6.60E-08	0.0412	1.80E-06	0.0229	2.62
20.4	0.043	2.2E-07	0.079	1.52E-06	0.0321	2.45	15.3	0.013	6.60E-08	0.0412	1.80E-06	0.0229	2.62
20.5	0.054	2.7E-07	0.079	1.52E-06	0.0321	2.45	15.4	0.013	6.60E-08	0.0412	1.80E-06	0.0229	2.62
150°C	1500 bar						16.1	0.101	5.13E-07	0.0753	3.29E-06	0.0231	2.62
							16.2	0.099	5.03E-07	0.0753	3.29E-06	0.0231	2.62
20.1	0.043	2.2E-07	0.079	1.76E-06	0.0322	2.31	16.3	0.102	5.18E-07	0.0753	3.29E-06	0.0231	2.62
20.2	0.042	2.1E-07	0.079	1.76E-06	0.0322	2.31	16.4	0.073	3.71E-07	0.0753	3.29E-06	0.0231	2.62
20.3	0.042	2.1E-07	0.079	1.76E-06	0.0322	2.31	16.5	0.088	4.47E-07	0.0753	3.29E-06	0.0231	2.62
20.4	0.044	2.2E-07	0.079	1.76E-06	0.0322	2.31							
20.5	0.043	2.2E-07	0.079	1.76E-06	0.0322	2.31	19.1	0.0023	1.17E-08	0.0326	7.29E-06	0.0229	3.33
							19.2	0.0023	1.17E-08	0.0326	7.29E-06	0.0229	3.33
							20.1	0.085	4.32E-07	0.0786	3.47E-06	0.023	2.65
							20.2	0.082	4.16E-07	0.0786	3.47E-06	0.023	2.65
							20.3	0.09	4.57E-07	0.0786	3.47E-06	0.023	2.65
	H2S-HS-												
22.1	33	0.00017	0.088	2.79E-02	0.0487	6.17	200°C	1000 bar					
22.2	31.1	0.00016	0.088	2.79E-02	0.0489	6.17							
23.1	5.78	2.9E-05	0.059	2.02E-02	0.0322	6.2	20.1	0.115	5.8E-07	0.0786	1.09E-06	0.0231	2.41
23.2	5.84	3E-05	0.059	2.02E-02	0.0322	6.2	20.2	0.108	5.5E-07	0.0786	1.09E-06	0.0231	2.41
							20.3	0.098	5E-07	0.0786	1.09E-06	0.0231	2.41
							20.4	0.129	6.5E-07	0.0786	1.09E-06	0.0231	2.41
24.1	10.187	5.2E-05	0.095	5.54E-03	0.202	5.43	200°C	1500 bar					
24.2	10.269	5.2E-05	0.095	5.54E-03	0.202	5.43							
24.3	9.765	5E-05	0.095	5.54E-03	0.202	5.43	20.1	0.125	6.3E-07	0.0786	1.33E-06	0.0231	2.28
24.4	9.316	4.7E-05	0.095	5.54E-03	0.202	5.43	20.2	0.107	5.4E-07	0.0786	1.33E-06	0.0231	2.28
							20.3	0.104	5.3E-07	0.0786	1.33E-06	0.0231	2.28
27.1	7.25	3.7E-05	0.045	3.46E-03	0.193	5.56							
27.2	7.262	3.7E-05	0.048	3.46E-03	0.193	5.53							
27.3	7.144	3.6E-05	0.048	3.46E-03	0.193	5.53							
27.4	7.249	3.7E-05	0.048	3.46E-03	0.193	5.53							
							200°C	H2S / HS- 500 bar					
28.1	2.751	1.4E-05	0.027	2.14E-03	0.18	5.58	21.1	61.8	3.14E-04	0.1	2.75E-02	0.15	6.44
28.2	2.855	1.4E-05	0.027	2.14E-03	0.18	5.58	21.2	60.98	3.10E-04	0.1	2.75E-02	0.15	6.44
28.3	2.733	1.4E-05	0.027	2.14E-03	0.18	5.58	21.3	61.748	3.13E-04	0.1	2.75E-02	0.15	6.44
28.4	2.899	1.5E-05	0.027	2.14E-03	0.18	5.58	21.4	62.427	3.17E-04	0.1	2.75E-02	0.15	6.44
28.5	3.005	1.5E-05	0.027	2.14E-03	0.18	5.58	21.5	59.567	3.02E-04	0.1	2.75E-02	0.15	6.44
							21.6	62.733	3.18E-04	0.1	2.75E-02	0.15	6.44
150°C	1000 bar						22.1	38.3	1.94E-04	0.0999	2.66E-02	0.102	6.43
							22.2	38	1.93E-04	0.0999	2.66E-02	0.102	6.43
28.1	2.303	1.2E-05	0.027	2.14E-03	0.179	5.44	23.1	7.97	4.05E-05	0.0153	2.29E-03	0.0392	6.18
28.2	2.276	1.2E-05	0.027	2.14E-03	0.179	5.44	23.2	8.19	4.16E-05	0.0153	2.29E-03	0.0396	6.18
28.3	2.416	1.2E-05	0.027	2.14E-03	0.179	5.44							
28.4	2.527	1.3E-05	0.027	2.14E-03	0.179	5.44							
150°C	1500 bar						27.1	11.352	5.76E-05	0.0453	3.41E-03	0.146	5.88
							27.2	11.313	5.74E-05	0.0453	3.41E-03	0.146	5.88
28.1	1.971	1E-05	0.027	2.13E-03	0.178	5.31	27.3	11.214	5.69E-05	0.0453	3.41E-03	0.146	5.88
28.2	1.991	1E-05	0.027	2.13E-03	0.178	5.31	27.4	11.139	5.66E-05	0.0453	3.41E-03	0.146	5.88
28.3	2.075	1.1E-05	0.027	2.13E-03	0.178	5.31							
28.4	2.146	1.1E-05	0.027	2.13E-03	0.178	5.31	28.1	4.103	2.08E-05	0.0267	2.11E-03	0.023	5.90
							28.2	4.164	2.11E-05	0.0267	2.11E-03	0.023	5.90
							28.3	4.131	2.10E-05	0.0267	2.11E-03	0.023	5.90
							28.4	4.005	2.03E-05	0.0267	2.11E-03	0.023	5.90
							200°C	1000 bar					
							28.1	3.493	1.8E-05	0.0267	2.11E-03	0.129	5.55
							28.2	3.482	1.8E-05	0.0267	2.11E-03	0.129	5.55
							28.3	3.294	1.7E-05	0.0267	2.11E-03	0.129	5.55
							28.4	3.28	1.7E-05	0.0267	2.11E-03	0.129	5.55
							200°C	1500 bar					
							28.1	2.765	1.4E-05	0.0267	2.11E-03	0.13	5.72
							28.2	2.737	1.4E-05	0.0267	2.11E-03	0.13	5.72
							28.3	2.955	1.5E-05	0.0267	2.11E-03	0.13	5.72
							28.4	2.864	1.5E-05	0.0267	2.11E-03	0.13	5.72

APPENDIX AII. Continued.

H2S or H2S/H3PO4 250°C 500 bar							H2S or H2S/H3PO4 300°C 500 bar						
run	Au(ppm)	mAu	aH2S	a HS-	fH2, tot	pH	run	Au(ppm)	mAu	aH2S	a HS-	fH2, tot	pH
1.1	0.792	4.02E-06	0.051	4.66E-05	0.0149	4.33	3.1	0.431	2.19E-06	0.092	4.41E-05	0.00759	4.35
1.4	0.859	4.36E-06	0.051	4.66E-05	0.015	4.33	3.2	0.587	2.98E-06	0.092	4.41E-05	0.00772	4.35
1.5	0.890	4.52E-06	0.051	4.66E-05	0.0151	4.33	3.3	0.487	2.47E-06	0.092	4.41E-05	0.00766	4.35
1.7	0.808	4.10E-06	0.051	4.66E-05	0.015	4.33	3.4	0.488	2.48E-06	0.092	4.41E-05	0.00766	4.35
1.8	0.938	4.76E-06	0.051	4.66E-05	0.0151	4.33	3.5	0.540	2.74E-06	0.092	4.41E-05	0.00769	4.35
1.9	0.920	4.67E-06	0.051	4.66E-05	0.015	4.33	3.6	0.546	2.77E-06	0.092	4.41E-05	0.0077	4.35
							3.7	0.516	2.62E-06	0.092	4.41E-05	0.00768	4.35
2.1	1.211	6.15E-06	0.079	5.83E-05	0.0154	4.23	4.1	0.165	8.38E-07	0.109	4.82E-06	0.00741	3.32
2.2	1.121	5.69E-06	0.079	5.83E-05	0.0154	4.23	4.2	0.178	9.04E-07	0.109	4.82E-06	0.0746	3.32
2.3	0.957	4.86E-06	0.079	5.83E-05	0.0152	4.23							
2.5	1.032	5.24E-06	0.079	5.83E-05	0.0153	4.23							
2.6	1.024	5.20E-06	0.079	5.83E-05	0.0152	4.23	5.1	0.050	2.54E-07	0.02	2.04E-05	0.00737	4.68
2.7	1.105	5.61E-06	0.079	5.83E-05	0.0153	4.23	5.2	0.045	2.28E-07	0.02	2.04E-05	0.00737	4.68
2.10	0.979	4.97E-06	0.079	5.83E-05	0.0152	4.23							
2.11	1.081	5.49E-06	0.079	5.83E-05	0.0153	4.23	6.1	0.180	9.14E-07	0.036	2.75E-05	0.00746	4.55
							6.2	0.151	7.67E-07	0.036	2.75E-05	0.00744	4.55
3.1	0.640	3.25E-06	0.092	6.30E-05	0.0147	4.20	6.3	0.103	5.23E-07	0.036	2.75E-05	0.00741	4.55
3.2	0.709	3.60E-06	0.092	6.30E-05	0.0149	4.20	6.4	0.086	4.37E-07	0.036	2.75E-05	0.00739	4.55
3.3	0.760	3.86E-06	0.092	6.30E-05	0.0149	4.20	6.5	0.075	3.81E-07	0.036	2.75E-05	0.00739	4.55
3.4	0.660	3.35E-06	0.092	6.30E-05	0.0148	4.20	6.6	0.149	7.56E-07	0.036	2.75E-05	0.00744	4.55
3.6	0.648	3.29E-06	0.092	6.30E-05	0.0148	4.20							
3.8	0.717	3.64E-06	0.092	6.30E-05	0.0149	4.20	8.1	0.187	9.49E-07	0.038	2.83E-05	0.00746	4.54
3.9	0.735	3.73E-06	0.092	6.30E-05	0.0148	4.20	8.2	0.182	9.24E-07	0.038	2.83E-05	0.00746	4.54
							8.3	0.189	9.60E-07	0.038	2.83E-05	0.00746	4.54
4.1	0.615	3.12E-06	0.109	6.87E-05	0.0147	4.16							
4.2	0.670	3.40E-06	0.109	6.87E-05	0.0148	4.16	9.1	0.073	3.71E-07	0.028	2.43E-05	0.00739	4.60
							9.2	0.069	3.50E-07	0.028	2.43E-05	0.00738	4.60
5.1	0.081	4.11E-07	0.02	2.92E-05	0.0141	4.52	9.3	0.055	2.79E-07	0.028	2.43E-05	0.00737	4.60
5.2	0.095	4.82E-07	0.02	2.92E-05	0.0141	4.52	9.4	0.058	2.94E-07	0.028	2.43E-05	0.00738	4.60
6.1	0.141	7.16E-07	0.036	3.93E-05	0.0141	4.40	11.1	0.148	7.51E-07	0.066	3.31E-06	0.00744	3.37
6.2	0.221	1.12E-06	0.036	3.93E-05	0.0142	4.40	11.2	0.161	8.17E-07	0.066	3.31E-06	0.00744	3.37
							11.3	0.117	5.94E-07	0.066	3.31E-06	0.00741	3.37
8.1	0.335	1.70E-06	0.038	4.05E-05	0.0144	4.38	11.4	0.161	8.17E-07	0.066	3.31E-06	0.00744	3.37
8.2	0.362	1.84E-06	0.038	4.05E-05	0.0144	4.38							
8.4	0.360	1.83E-06	0.038	4.05E-05	0.0144	4.38	12.1	0.299	1.52E-06	0.066	3.44E-06	0.00754	3.39
8.5	0.347	1.76E-06	0.038	4.05E-05	0.0144	4.38	12.2	0.295	1.50E-06	0.066	3.44E-06	0.00753	3.39
8.6	0.333	1.69E-06	0.038	4.05E-05	0.0144	4.38							
							13.1	0.001	1.50E-06	0.024	3.19E-07	0.00734	2.79
9.1	0.063	3.20E-07	0.028	3.48E-05	0.014	4.45	13.2	0.001	1.50E-06	0.024	3.19E-07	0.00734	2.79
9.2	0.063	3.20E-07	0.028	3.48E-05	0.014	4.45							
9.3	0.060	3.05E-07	0.028	3.48E-05	0.014	4.45	14.1	0.029	1.47E-07	0.011	1.48E-05	0.00736	4.81
9.4	0.060	3.05E-07	0.028	3.48E-05	0.014	4.45	14.2	0.049	2.49E-07	0.011	1.48E-05	0.00737	4.81
							14.3	0.032	1.62E-07	0.011	1.48E-05	0.00736	4.81
10.1	0.063	3.20E-07	0.045	2.65E-06	0.014	3.13	14.4	0.031	1.57E-07	0.011	1.48E-05	0.00736	4.81
10.2	0.073	3.71E-07	0.045	2.65E-06	0.0141	3.13							
10.3	0.057	2.89E-07	0.045	2.65E-06	0.014	3.13	16.1	0.076	3.86E-07	0.075	3.36E-07	0.00739	2.32
10.4	0.063	3.20E-07	0.045	2.65E-06	0.014	3.13	16.2	0.078	3.96E-07	0.075	3.36E-07	0.00739	2.32
							16.3	0.069	3.50E-07	0.075	3.36E-07	0.00738	2.32
11.1	0.166	8.43E-07	0.066	5.37E-06	0.0142	3.27	16.4	0.069	3.50E-07	0.075	3.36E-07	0.00738	2.32
11.2	0.150	7.62E-07	0.066	5.37E-06	0.0142	3.27	16.5	0.070	3.55E-07	0.075	3.36E-07	0.00738	2.32
11.4	0.165	8.38E-07	0.066	5.37E-06	0.0142	3.27	16.6	0.074	3.76E-07	0.075	3.36E-07	0.00739	2.32
11.5	0.142	7.21E-07	0.066	5.37E-06	0.0141	3.27	16.7	0.070	3.55E-07	0.075	3.36E-07	0.00738	2.32
12.1	0.230	1.17E-06	0.066	5.57E-06	0.0144	3.29	19.1	0.003	3.55E-07	0.033	2.15E-06	0.00734	3.49
12.2	0.228	1.16E-06	0.066	5.57E-06	0.0144	3.29	19.2	0.003	3.55E-07	0.033	2.15E-06	0.00734	3.49
13.1	0.002	1.16E-06	0.024	4.94E-07	0.014	2.67	20.1	0.059	3.00E-07	0.079	4.12E-07	0.00738	2.39
13.2	0.002	1.16E-06	0.024	4.94E-07	0.014	2.67	20.2	0.075	3.81E-07	0.079	4.12E-07	0.00739	2.39
							20.3	0.070	3.53E-07	0.079	4.12E-07	0.00738	2.39
14.1	0.063	3.20E-07	0.011	2.13E-05	0.014	4.65							
14.2	0.057	2.89E-07	0.011	2.13E-05	0.014	4.65							
14.3	0.065	3.30E-07	0.011	2.13E-05	0.014	4.65	300°C		1000 bar				
14.4	0.064	3.25E-07	0.011	2.13E-05	0.014	4.65	20.1	0.094	4.8E-07	0.079	6.19E-07	0.0074	2.25
							20.2	0.091	4.6E-07	0.079	6.19E-07	0.0074	2.25
16.1	0.117	5.94E-07	0.075	8.85E-07	0.0141	2.43	20.3	0.083	4.2E-07	0.079	6.19E-07	0.0074	2.25
16.2	0.117	5.94E-07	0.075	8.85E-07	0.0141	2.43	20.4	0.094	4.8E-07	0.079	6.19E-07	0.0074	2.25
16.3	0.114	5.79E-07	0.075	8.85E-07	0.0141	2.43							

Appendix A III. A summary of the thermodynamic data and their sources

Reactions	Log K						data
	150°C	200°C	250°C	300°C	350°C	400°C	source
$H_{2(g)} \rightleftharpoons H_{2(aq)}$ at swvp	-2.98	-2.81	-2.61	-2.38	-2.07	-	1
$H_{2(g)} \rightleftharpoons H_{2(aq)}$ at 500 bar	-3.15	-2.97	-2.76	-2.54	-2.28	-1.96	
$H_{2(g)} \rightleftharpoons H_{2(aq)}$ at 1000 bar	-3.32	-3.13	-2.91	-2.69	-2.45	-2.19	
$H_{2(g)} \rightleftharpoons H_{2(aq)}$ at 1500 bar	-3.49	-3.28	-3.06	-2.82	-2.59	-2.24	
$H_2O \rightleftharpoons H^+ + OH^-$ at 500 bar	-11.45	-11.05	-10.85	-10.86	-11.14	-11.88	2
$H_2O \rightleftharpoons H^+ + OH^-$ at 1000 bar	-11.29	-10.86	-10.60	-10.50	-10.54	-10.77	
$H_2O \rightleftharpoons H^+ + OH^-$ at 1500 bar	-11.16	-10.71	-10.43	-10.26	-10.22	-10.29	
$H_2S_{(aq)} \rightleftharpoons HS^- + H^+$ at swvp	-6.82	-7.20	-7.61	-8.00	-8.31	-	3
$H_2S_{(aq)} \rightleftharpoons HS^- + H^+$ at 500 bar	-6.67	-6.98	-7.36	-7.67	-7.88	-7.96	
$H_2S_{(aq)} \rightleftharpoons HS^- + H^+$ at 1000 bar	-6.53	-6.83	-7.10	-7.31	-7.39	-7.31	
$H_2S_{(aq)} \rightleftharpoons HS^- + H^+$ at 1500 bar	-6.40	-6.66	-6.86	-6.98	-6.96	-6.76	
$Na^+ + HS^- \rightleftharpoons NaHS^{\circ}$ at 500 bar	-0.31	-0.04	0.27	0.64	1.15	1.69	4
$Na^+ + HS^- \rightleftharpoons NaHS^{\circ}$ at 1000 bar	-0.38	-0.14	0.13	0.42	0.75	1.12	
$Na^+ + HS^- \rightleftharpoons NaHS^{\circ}$ at 1500 bar	-0.43	-0.21	0.03	0.28	0.55	0.85	
$H_3PO_4 \rightleftharpoons H_2PO_4^- + H^+$ at 500 bar	-2.71	-3.03	-3.27	-3.55	-3.83	-4.11	5
$H_3PO_4 \rightleftharpoons H_2PO_4^- + H^+$ at 1000 bar	-2.58	-2.89	-3.14	-3.41	-3.69	-3.96	
$H_3PO_4 \rightleftharpoons H_2PO_4^- + H^+$ at 1500 bar	-2.47	-2.76	-3.01	-3.27	-3.53	-3.80	
$Au^+ + 1/2 H_{2(g)} \rightleftharpoons Au_{(s)} + H^+$ at 500 bar	-18.29	-15.68	-13.57	-11.83	-10.37	-9.12	6
$Au^+ + 1/2 H_{2(g)} \rightleftharpoons Au_{(s)} + H^+$ at 1000 bar	-18.31	-15.69	-13.58	-11.83	-10.35	-9.10	
$Au^+ + 1/2 H_{2(g)} \rightleftharpoons Au_{(s)} + H^+$ at 1500 bar	-18.33	-15.71	-13.59	-11.83	-10.35	-9.10	

(1) SUPCRT92 (JOHNSON *et al.*, 1992); (2) MARSHALL and FRANCK (1981); (3) up to 276°C ELLIS and GIGGENBACH (1971), above extrapolated, pressure corrections to 1500 bar using the partial molar volume data from ELLIS and MCFADDEN (1972); (4) in analogy to $NaCl^{\circ}$ after SHOCK *et al.* (1992); (5) up to 200°C READ (1988), above extrapolated; (6) SUPCRT92 (JOHNSON *et al.*, 1992).